Progress in Retinal and Eye Research 29 (2010) 59–78

Contents lists available at ScienceDirect

Progress in Retinal and Eye Research

journal homepage: www.elsevier.com/locate/prer

A mass and solute balance model for tear volume and osmolarity in the normal and the dry eye

E.A. Gaffney [a,b,*], J.M. Tiffany [c], N. Yokoi [d], A.J. Bron [c]

[a] Centre for Mathematical Biology, Mathematical Institute, University of Oxford, UK
[b] Oxford Centre for Collaborative Applied Mathematics, Mathematical Institute, University of Oxford, UK
[c] Nuffield Laboratory of Ophthalmology, Medical Sciences Division, University of Oxford, John Radcliffe Hospital, Oxford, UK
[d] Department of Ophthalmology, Kyoto Prefectural University of Medicine, Kyoto, Japan

Keywords:
Tear film
Tear volume
Tear osmolarity
Tear hyperosmolarity
Compartment model

A B S T R A C T

Tear hyperosmolarity is thought to play a key role in the mechanism of dry eye, a common symptomatic condition accompanied by visual disturbance, tear film instability, inflammation and damage to the ocular surface. We have constructed a model for the mass and solute balance of the tears, with parameter estimation based on extensive data from the literature which permits the influence of tear evaporation, lacrimal flux and blink rate on tear osmolarity to be explored. In particular the nature of compensatory events has been estimated in aqueous-deficient (ADDE) and evaporative (EDE) dry eye.

The model reproduces observed osmolarities of the tear meniscus for the healthy eye and predicts a higher concentration in the tear film than meniscus in normal and dry eye states. The differential is small in the normal eye, but is significantly increased in dry eye, especially for the simultaneous presence of high meniscus concentration and low meniscus radius. This may influence the interpretation of osmolarity values obtained from meniscus samples since they need not fully reflect potential damage to the ocular surface caused by tear film hyperosmolarity.

Interrogation of the model suggests that increases in blink rate may play a limited role in compensating for a rise in tear osmolarity in ADDE but that an increase in lacrimal flux, together with an increase in blink rate, may delay the development of hyperosmolarity in EDE. Nonetheless, it is predicted that tear osmolarity may rise to much higher levels in EDE than ADDE before the onset of tear film breakup, in the absence of events at the ocular surface which would independently compromise tear film stability. Differences in the predicted responses of the pre-ocular tears in ADDE compared to EDE or hybrid disease to defined conditions suggest that no single, empirically-accessible variable can act as a surrogate for tear film concentration and the potential for ocular surface damage. This emphasises the need to measure and integrate multiple diagnostic indicators to determine outcomes and prognosis. Modelling predictions in addition show that further studies concerning the possibility of a high lacrimal flux phenotype in EDE are likely to be profitable.

Contents

* Corresponding author. Centre for Mathematical Biology, Mathematical Institute, University of Oxford, UK.
E-mail address: gaffney@maths.ox.ac.uk (E.A. Gaffney).

1350-9462/$ – see front matter © 2009 Elsevier Ltd. All rights reserved.
doi:10.1016/j.preteyeres.2009.11.002

1. Introduction

The tear fluid is distributed over the ocular surface and occupies three compartments. The first two are the menisci and the tear film which together make up the pre-ocular fluid. This is exposed to the atmosphere when the eyes are open. The third consists of fluid in the retro-tarsal spaces in continuity with that in the conjunctival fornices. For convenience this will be referred to as the *fornical fluid*. Aqueous tears are secreted into the supero-lateral fornix by the main and palpebral portions of the lacrimal gland and into the upper fornix by the accessory lacrimal glands; there is a small conjunctival contribution. Fluid is lost by drainage via the nasolacrimal system and by evaporation from the exposed tear surface.

The tear film is refreshed by blinking, which in normal subjects occurs with a frequency of between 10 and 30 per minute (Tomlinson and Khanal, 2005). The blink cycle consists of the upstroke and downstroke of the blink, taking between 0.2 and 0.27 s (Tsubota et al., 1996), and the interblink period whose length depends on the blink rate. During the blink there is limited mixing of fluids between the menisci and the fornical compartments (MacDonald and Maurice, 1991), and during the interblink there is also postulated flow between the compartments. In the upstroke of the blink, meibomian lipid is drawn upwards over the aqueous subphase of the tear film to form a stable tear film lipid layer (Goto and Tseng, 2003; Owens and Phillips, 2002).

Tear dynamics are regulated by a feedback system involving a reflex arc between the ocular surface, brainstem and the lacrimal glands. This is termed the Lacrimal Functional Unit (Stern et al., 2004, 1998a,b; Pflugfelder et al., 2000; DEWS, 2007a; Beuerman et al., 2004). There are additional inputs from the nasolacrimal system and higher centres of the brain. Its overall role is to preserve the health of the ocular surface. In the waking state tear flow is maintained by afferent impulses from the exposed surface of the eye; irritation of the ocular surface leads to an increase in sensory drive and thus lacrimal secretion while blockade of either the afferent or efferent limbs of the reflex arc leads to a decrease in lacrimal secretion.

Dry eye is a common and mainly age-related affliction responsible for considerable disability and time off work, and occurs in 5.5–34% of the over 65 s, according to the method of measurement, or geographic location (DEWS, 2007b).

The condition was redefined at the recent international dry eye workshop, DEWS 2007, (DEWS, 2007a): "Dry eye is a multifactorial disease of the tears and ocular surface that results in symptoms of discomfort, visual disturbance, and tear film instability, with potential damage to the ocular surface (Adatia et al., 2004; Begley et al., 2004; Vitale et al., 2004; Rieger, 1992; Liu and Pflugfelder, 1999; Goto et al., 2002; Holly and Lemp, 1973; Bron, 2001; Goto and Tseng, 2003; Farris et al., 1986; Gilbard, 1994; Murube, 2006; Tomlinson et al., 2006). It is accompanied by increased osmolarity of the tear film and inflammation of the ocular surface (Pflugfelder et al., 1999; Tsubota et al., 1999)." The workshop also confirmed the utility of recognizing two major forms of dry eye disease, aqueous-deficient dry eye, due to a reduced secretion of aqueous tears (ADDE) and evaporative dry eye due to excessive evaporative water loss from the exposed ocular surface (EDE) (Lemp, 1995; DEWS, 2007a).

Dry eye induced tear hyperosmolarity is recognised as a major cause of ocular surface damage (Gilbard et al., 1984, 1989; Huang et al., 1989; Baudouin, 2007). Consequently, it is important to understand how tear osmolarity varies across the whole ocular surface even though the clinical picture is influenced by other factors such as ocular surface inflammation and lid abnormalities. However, assessing the relationship between tear meniscus osmolarity and the potential for ocular surface damage is hindered by the technical difficulty of measuring osmolarity directly in the tear film or in the epithelium of the exposed ocular surface itself, although some approaches have been have been reported (Gupta et al., 2006).

To address this, the quantitative modelling presented here utilises existing data and concepts (Bron et al., 2002), with a generalization of current compartment models (Worakul and Robinson, 1997; Zhu and Chauhan, 2007) to specifically investigate the factors modifying hyperosmolarity in dry eye. Such a modelling investigation will allow us to approximate and delimit the overall behaviour

of solute concentrations within each tear compartment and to investigate their relevance to dry eye. The main foci of this paper are:

- What diagnostic measures will indicate the presence of an elevated tear film osmolarity?
- On comparing evaporative and aqueous-deficient dry eye, is there any difference in the pattern or extent of hyperosmolarity that will emerge as these pathologies progress?
- In the presence of dry eye, are there compensatory mechanisms driven by a feedback between hyperosmolarity of the ocular surface and both the blink rate and the lacrimal gland flux?
- To what extent could such compensation ameliorate high ocular surface osmolarities for different types of dry eye?

These have important implications for understanding how the potential for ocular surface damage caused by tear hyperosmolarity influences dry eye diagnosis.

While there has been significant work modelling the fluid and solute dynamics of the tear film, this has not focussed on such questions. For example, lubrication theory models of the flow between blinks have been considered (Sharma et al., 1998; Braun and Fitt, 2003; Wong et al., 1996). The former two focussed on tear breakup times, emphasising the importance of evaporation and gravity, while the latter investigated tear deposition in the upstroke of the blink. A global balance model, treating the ocular surface fluid as a single compartment, has also been developed and investigated for the mouse eye (Levin and Verkman, 2004). In addition, aspects of the mixing and drainage of tears have been modelled together with the development of a compartmental model of tear balance (Zhu and Chauhan, 2005a,b, 2007). However, such models have not considered solute balance and the ocular surface fluids in sufficient detail to enable a modelling interrogation of the above questions.

Previously, in a conceptual model, we predicted that regional variations of tear osmolarity exist over the ocular surface that may determine the distribution of ocular surface damage in dry eye and hypothesized that, in the waking state, tear osmolarity is influenced by a compartmentalization of tears at the ocular surface (Bron et al., 2002). It was proposed that

1. The osmolarity of the meniscal and tear film fluids is not identical
2. The osmolarity of the tear film always exceeds that of the meniscus
3. This differential is amplified in dry eye states.

This framework is generalised in a consistent manner to yield a quantitative model, which we develop and justify in the next section, paying particular attention to the relation between parameter estimation and current empirical data.

2. Mass and solute balance model for the tear film

In the following, we develop our modelling framework using mass and solute balance for the ocular surface fluid. This is simply the statement that fluid and solute are conserved. Thus, for example, mass balance demands that the rate of change of volume of a given compartment is the sum of the volume fluxes (that is volume transferred per unit time) into the compartment, minus the sum of the volume fluxes out of the compartment. Immediately below we develop a model for the tear film in the interblink, i.e. between blinks, followed by detailed parameter estimations, before finally we consider mass and solute balance in the blink phase.

2.1. The model for the interblink

We consider a simple representation of the ocular surface fluid occupying the following compartments

- The meniscus
- The tear film,

together making up the exposed pre-ocular fluid, plus

- The conjunctival (fornical) sac fluid, representing the fluid lying in the fornices and retro-tarsal spaces.

Noting that

- V_m denotes the meniscus volume.
- V_{tf} denotes the tear film volume.
- V_f denotes volume of fluid in the conjunctival (fornical) sac

We can readily write down mass balance equations during the interblink in terms of fluxes between the compartments; see Fig. 1 for a schematic depiction. For example, the rate of change of the meniscus volume, i.e. dV_m/dt, is the sum of the volume flux of fluid into the meniscus from the tear film and the volume flux of fluid into the meniscus from the fornical sac minus the volume flux due to drainage and due to evaporation. The latter is simply the volumetric evaporation rate per unit surface area multiplied by the meniscus surface area. Hence

$$\begin{aligned}\frac{dV_m}{dt} &= [\text{Flux from tear film to meniscus}] \\ &\quad - [\text{Meniscus surface area}] \times [\text{Evaporation rate}] \\ &\quad - [\text{Drainage flux}] + [\text{Flux from fornical sac}].\end{aligned}$$

Analogously, we have

$$\begin{aligned}\frac{dV_{tf}}{dt} &= -[\text{Tear film surface area}] \times [\text{Evaporation rate}] \\ &\quad -[\text{Flux from tear film to meniscus}], \\ \frac{dV_f}{dt} &= -[\text{Flux from fornical sac}] + [\text{Flux from lacrimal gland}].\end{aligned}$$

The equations describing solute balance can be derived similarly. First note that

- Q_m denotes the osmolar amount of solute in the meniscus
- Q_{tf} denotes the osmolar amount of solute in the tear film
- Q_f denotes the osmolar amount of solute in the fornical sac.

Then, for example, the rate of change of the solute in the meniscus, i.e. dQ_m/dt, is the sum of the solute fluxes into the meniscus from the tear film and from the fornical sac minus the solute flux due to drainage. In turn the solute flux into the meniscus from the tear film is the volume flux of fluid multiplied by the concentration of solute in the tear film; the latter is simply Q_{tf}/V_{tf}. Similarly for the other solute fluxes, yielding the solute balance equation

$$\begin{aligned}\frac{dQ_m}{dt} &= [\text{Flux from tear film to meniscus}] \times \frac{Q_{tf}}{V_{tf}} \\ &\quad + [\text{Flux from fornical sac}] \times \frac{Q_f}{V_f} - [\text{Drainage flux}] \times \frac{Q_m}{V_m}.\end{aligned}$$

The other solute balance equations are derived analogously to give

$$\begin{aligned}\frac{dQ_{tf}}{dt} &= -[\text{Flux from tear film to meniscus}] \times \frac{Q_{tf}}{V_{tf}}, \\ \frac{dQ_f}{dt} &= -[\text{Flux from fornical sac}] \times \frac{Q_f}{V_f} \\ &\quad +[\text{Flux from lacrimal gland}] \\ &\quad \times[\text{Concentration of solute in fluid from lacrimal gland}].\end{aligned}$$

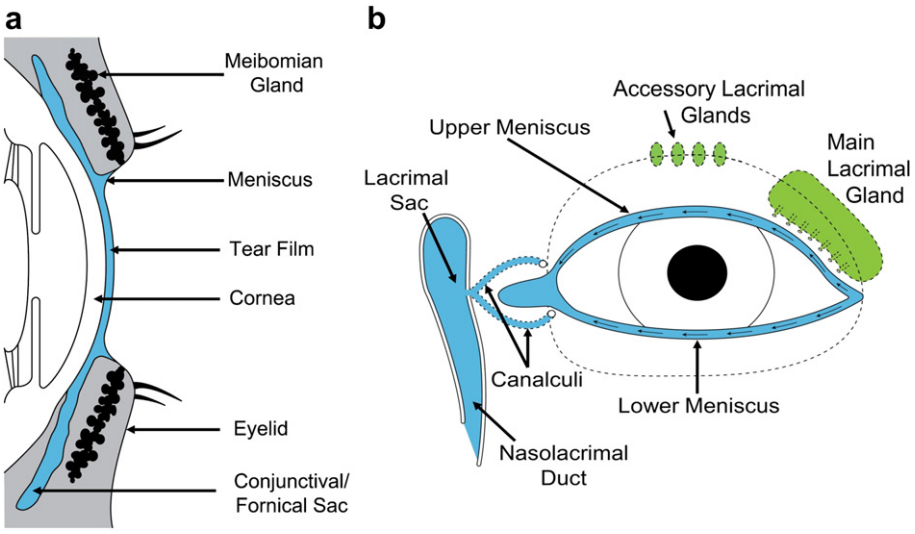

Fig. 1. a (left): Sagittal view of the eye to show tear distribution. b (right): Schematic view of the lacrimal drainage system. Tears flow from the main and accessory lacrimal glands into the conjunctival sac and thence into the tear menisci. The negative hydrostatic pressure in the menisci draws fluid from the tear film into the menisci during the interblink period; during the start of the interblink fluid flows from the menisci via the upper and lower punctal openings into the canaliculi and thence into the lacrimal sac. From there the tears flow into the nasolacrimal duct where they are either absorbed or continue into the nasal passages. (See text for details of the factors influencing tear flow and drainage).

The reader may notice that the effects of diffusion, that is the movement of solutes down concentration gradients, are neglected in the above; the justification for this is presented in the appendix.

2.1.1. The parameters for the interblink model

2.1.1.1. The healthy eye. The ordinary differential equations given above depend on numerous parameters; however the number of degrees of freedom is far less than the number of parameters due to relationships between the latter. Below, we discuss parameter estimation, taking into account these constraints. The outcome of this subsection is summarised in Table 1 where a list of reference parameter values is given for the healthy eye. All parameters in the text are quoted in SI units, which are used throughout this paper because of their self-consistency. A conversion to units frequently used in the ophthalmological literature is also presented in Table 1.

2.1.1.2. Interblink time. This is the time between blinks and is reported to be 4 ± 2 s in normal individuals and 1.5 ± 0.9 s in dry eye individuals (Tomlinson and Khanal, 2005; Tsubota et al., 1996; Tsubota, 1998). For the representative parameters of the healthy eye we simply take this time to be 4.0 s. Dry eye may increase the blink rate through a reflex feedback loop, so we will additionally investigate the effect of shortening the interblink time to 1.6 s, as well as varying the interblink time, in our simulations.

2.1.1.3. Geometrical parameters. A fundamental measurable parameter is the meniscus radius of curvature, which is denoted as a_1. As will be discussed below, this is a surrogate for total tear volume and lacrimal flux. It also determines the area of the meniscus exposed to evaporative water loss. This parameter has been determined to have a mean and standard deviation of 3.65e-4 m and 1.5e-4 m (Yokoi et al., 1999) for the normal eye. We have explicitly varied this parameter in our detailed simulations, considering a very wide range, encompassing extremes in the observed range to account for the variation reported empirically.

Two further key parameters for the meniscus are the meniscus depth, denoted q, and the meniscus height, denoted h_0, as illustrated in Fig. 2. The parameters a_1, q, h_0 are related by elementary geometry (see Fig. 2)

$$h_0^2 + (a_1 - q)^2 = a_1^2, \quad \text{i.e.} \quad q^2 - 2a_1 q + h_0^2 = 0, \tag{1}$$

on the assumption that the tear film thickness is much smaller than these parameters and that the meniscus profile can be approximated by a circular arc. The former is clearly true. The latter has been confirmed empirically (Yokoi et al., 1999), even for large meniscus volumes achieved by injecting fluid into the meniscus (JM Tiffany, unpublished). The meniscus depth, q, is the distance from the muco-cutaneous junction to the ocular surface and corresponds to the width of the marginal strip of the lid mucosa. For a given individual it represents the full extent of the wettable mucosal surface of the lid as the lid skin anterior to the muco-cutaneous junction is hydrophobic. Thus, it is not affected by an increase in meniscus volume up to the point where excessive volume leads to a brimming over of the tears. Hence, while the meniscus depth can and probably does vary between individuals, it can be considered to be constant on varying the quantity of lacrimal fluid and the evaporation rates below.

To estimate the meniscus depth, we explicitly consider empirical measures of the mean meniscus height, h_0. Surveying the literature, this parameter is reported with a mean of 2.8e-4 m (Johnson and Murphy, 2005). However, improved measurements indicate that this is an underestimate due to difficulties in resolving the central edge of the meniscus (*ibid*); the mean of measurements made by the above authors ranged from 3.1e-4 m to 3.8e-4 m according to measurement techniques. One must have $h_0 \leq a_1$ for consistency. Thus, solving equation (1) for q, with $a_1 = 3.65$e-4 m and h_0 taking values between 3.1e-4 m and 3.65e-4 m, we have that q lies between the values 1.72e-4 m and 3.65e-4 m. In our simulations, we estimate q to be 2.7e-4 m, the two significant figure midpoint of this range.

As stated above, the parameter q is constant for a given individual as we vary either the meniscus radius of curvature or the evaporation rate. Thus, in general, the meniscus height is given by $h_0 = \sqrt{a_1^2 - (q - a_1)^2}$ as we vary parameters in our simulations. Analogously, the mean meniscus cross sectional area, C, and the length of the meniscus–air interface along this cross section, L, are then given by

Table 1
A reference set of physical parameters influencing tear dynamics for the healthy eye. All units in this table and throughout the paper are SI units, but for convenience values are also given here in units commonly reported in the ophthalmological literature. Note that in SI units, time is measured in seconds, length in metres, mass in kilograms, osmolarity in Osmoles per cubic metre. The volume parameters, V_{tf}^0, V_f^0, V_m^0 describe volumes at the start of the interblink. Many parameters are derived as discussed in the text. The parameter λ is described below in the section on blinking.

Parameter	Value SI units	Value commonly used units	Comments
Interblink Time, T (Time between blinks)	4.0 s	4.0 s	Measured. Tsubota et al. (1996) and Tsubota (1998)
Meniscus radius of Curvature, a_1	3.65e-4 m	0.365 mm, 365 μm	Measured, Yokoi et al. (1999)
Meniscus depth, q	2.7e-4 m	0.27 mm, 270 μm	Derived; see text and Johnson and Murphy (2005), Tiffany et al. (1997), Tsubota and Nakamori (1995)
Meniscus surface area, A_m^0	2.6e-5 m^2	26 mm^2	Derived. See text. Johnson and Murphy (2005)
Meniscus volume, V_m^0	1.34e-9 m^3	1.34 μl	Derived. See text
Perimeter of eyelid, P	5.4e-2 m	54 mm	Measured/Derived; see text. Tsubota and Nakamori (1995), Tiffany et al. (1997) and Mishima et al. (1966)
Tear film surface area	2.2e-4 m^2	220 mm^2	Tsubota and Nakamori (1995)
Tear film depth	3.0e-6 m	3.0 μm	Proportional to a_1. See text and King-Smith et al. (2000), Wong et al. (1996)
Tear film volume, V_{tf}^0	6.6e-10 m^3	0.66 μl	Height × Area
Fornical sac volume, V_f^0	5.0e-9 m^3	5.0 μl	Derived. See text
Evaporation Rate	4e-9 m s^{-1}	4e-7 g cm^{-2} s^{-1}	Observation. Goto et al. (2003). Density 1 g cm^{-3} assumed
Flux from tear to meniscus	5.58e-11 m^3 s^{-1}	0.0558 μl s^{-1}	See text
Drainage flux	5.37e-11 m^3 s^{-1}	0.0537 μl s^{-1}	Derived, see text and Tomlinson et al. (2001b), Zhu and Chauhan (2005b)
Drainage time	2.0 s	2.0 s	See text
Flux from lacrimal gland	2.81e-11 m^3 s^{-1}	0.0281 μl s^{-1}	Derived. See text
Flux from fornical sac	4.7e-12 m^3 s^{-1}	0.0047 μl s^{-1}	Derived. See text
Concentration of solute in-fluid from lacrimal gland	302 Osm m^{-3}	302 mOsm l^{-1}	Isotonic Secretion. Gilbard et al. (1978)
Proportion of mixing, λ	{0, 0.5, 1}	{0, 0.5, 1}	See text

$$C = \int_0^{h_0} dx \left[a_1 - \sqrt{a_1^2 - (x-h_0)^2} \right] = a_1 h_0 - \frac{h_0}{2}\sqrt{a_1^2 - h_0^2} - \frac{1}{2}a_1^2 \sin^{-1}\left(\frac{h_0}{a_1}\right),$$

$$L = \int_0^{h_0} dx \sqrt{1 + \frac{(x-h_0)^2}{a_1^2 - (x-h_0)^2}} = a_1 \sin^{-1}\left(\frac{h_0}{a_1}\right). \qquad (2)$$

Multiplying by the perimeter of the eyelid at the start of the interblink, P, gives an estimate for the total meniscus volume and the meniscus surface area (at the start of the interblink). Hence we take the meniscus volume and surface area at the start of each interblink to be given by

$$V_m^0 = PC, \quad A_m^0 = PL.$$

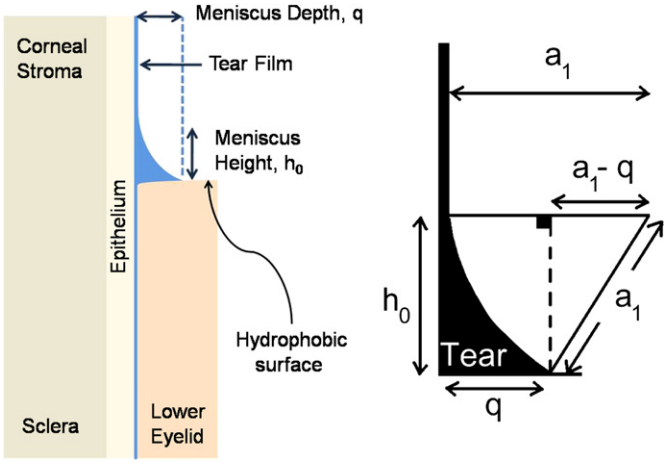

Fig. 2. The figure on the left depicts the definition of meniscus depth, q, and meniscus height, h_0. The figure on the right shows how one can relate the meniscus radius of curvature a_1, the meniscus depth, q, and the meniscus height, h_0.

Given the palpebral aperture is approximately elliptical, the area of the exposed globe is between 1.8e-4 m^2 and 2.6e-4 m^2 and the inter-palpebral height is between 9e-3 m and 1.1e-2 m (Tsubota and Nakamori, 1995; Tiffany et al., 1997), the perimeter lies in the range 4.9e-2 m–5.9e-2 m. For definiteness we use the mean perimeter P = 5.4e-2 m, which is also within 5% of independent estimates reported previously in the literature (Mishima et al., 1966).

Above we are predicting the value of the meniscus surface area at the start of the interblink, whereas for the calculation of evaporation rates we strictly need the mean meniscus surface area. The difference is assumed to be small, based on the fact that in some studies the meniscus radius of curvature is observed to be stable during the interblink (Yokoi et al., 1999). Other studies have suggested that the meniscus radius does increase by roughly 20% during the first 1.5 s following a blink (Johnson and Murphy, 2006), so that this assumption may induce a small error in the calculation of evaporative loss from the meniscus. However, the error is small, at the level of a few percent, since the overall evaporative loss from the meniscus is an order of magnitude less than the loss from the tear film, due to the much greater surface area of the latter. Similarly, its effect on the calculation of meniscus volume and solute concentration is always less than one percent, even for the smallest meniscus volumes, as the evaporative volume loss from the meniscus during the interblink is at least two orders of magnitude less than the meniscus volume. Thus, a time-varying treatment of the meniscus surface area is not considered because of the aim to keep the model as simple as possible while capturing the important transport physics.

Similarly, the tear film area will not be exactly constant during the blink, due to the action of capillary forces at the meniscus-tear film boundary. However, the area where such forces lead to an evolution of the tear film shape are small compared to the area of the tear film as a whole and treating the tear film surface area as constant is an excellent approximation. We use 2.2e-4 m^2 (Tsubota and Nakamori, 1995).

There is a wide variation in the reported thickness of the tear film even in the normal eye in the primary position of gaze. As reviewed by King-Smith et al. (2004) thicknesses ranging between 4e-5 m and 3e-6 m have been respectively reported

(Prydal et al., 1992; King-Smith et al., 2000), though the latter is now generally accepted. We will take a reference parameter thickness of 3e-6 m, following the most recent measurements. To consider how the tear film thickness will change with meniscus radius of curvature and thus lacrimal function, we consider the lubrication theory approximation. This proposes that the depth of the tear film at the start of the interblink is given by (Wong et al., 1996)

$$2.12a_1\left(\frac{\mu U}{\sigma}\right)^{2/3}, \tag{3}$$

where μ, σ are the tear film viscosity and surface tension, and with U denoting the speed of the blink upstroke. For typical values this yields a tear film thickness which is an overestimate, being of the order of 1e-5 m. Thus we still consider a tear film thickness which is proportional to the meniscus radius of curvature, but with a constant chosen such that the tear film thickness is 3e-6 m for the mean radius of curvature quoted above, namely 3.65e-4 m.

The fornical sac volume is determined by taking a representative value of the total volume of the ocular surface fluid and subtracting the tear and meniscus volumes. We work with the total volume 7.0e-9 m^3 (Tomlinson et al., 2001a; Tomlinson and Khanal, 2005). For the representative parameter values, this entails that the fornical sac volume is 5.0e-9 m^3 (two significant figures).

2.1.1.4. Osmolarity parameters. The lacrimal secretion is generally regarded to be isotonic (Gilbard et al., 1978) and the concentration is thus taken to be 302 Osm m^{-3} in the model. Hence there is no *a priori* conservation of total solute level in this model; if the amount of solute leaving via the canaliculi per unit time is different from the amount of solute entering the system from the lacrimal gland per unit time, then the net level of solute will change. Nonetheless, the system is observed below to asymptote to a periodic behaviour with volume and solute levels in one blink–interblink interval identical to the next and we are predominantly interested in this large time asymptote.

2.1.1.5. The contribution of the conjunctiva to tear secretion. Both the conjunctival epithelial cells and the goblet cells of the conjunctiva secrete a fluid which contributes to the total tear volume and flux. The physiological control of this secretion has been reviewed by Dartt (2002, 2005). This volume is neglected in the model on the basis of observations that this flux is small for the healthy eye (Tomlinson and Khanal, 2005; Khanal et al., 2008).

2.1.1.6. Flux parameters. The drainage flux represents the flux from the meniscus into the lacrimal drainage ducts. Evidence for this flux arises from the observation of carbon and other particles instilled into the lower meniscus (Dilly et al., 1998). However it has not been established whether this flow continues throughout the interblink period; here, we model the drainage flux as active for only a fixed interval of the interblink time. For the reference parameters in Table 1, we take it that the drainage flux is in effect for 2 s (Doane, 1981), which is 50% of the tabulated normal interblink duration. This flux is also considered to be permanently active when we consider interblink times of 2 s or less.

A driver of fluid from the meniscus into the nasolacrimal system was proposed under the name of the "lacrimal pump". This assumes that adduction of the eyes or orbicularis contraction during the blink or forced eye closure, compresses the lacrimal sac. The negative pressure resulting from the subsequent expansion of the lacrimal sac is transmitted to the tear menisci at the start of the interblink, resulting in drainage (Doane, 1981; Pavlidis et al., 2002). Here, instead we use the model of Zhu and Chauhan (2005a,b), where drainage is driven by the pressure difference between the meniscus and the canaliculi after a blink. This yields the prediction that the average drainage flux, denoted a_4 below, is given in terms of the meniscus radius of curvature, a_1, via

$$a_4 = \frac{\text{Interblink time}}{\text{Drainage time}} \times \frac{1}{\text{Interblink time}} \times 2.357 \times 10^{-9} \times \left\{ \frac{1}{\left(1+\frac{1.075\times 10^{-5}}{E^2 a_1^2}\right)} - \frac{1}{\left(1+\frac{10^{-1}}{E^2}\right)} \right\},$$

where the numerical values in the equations are given via the parameter estimates explicitly stated and used by Zhu and Chauhan (2005a,b). These depend upon the length and radius of the canaliculi, the surface tension, and the pressure difference between the lacrimal sac and the canaliculi due to the action of muscles surrounding the canaliculi (Pavlidis et al., 2002); see Table 2.

Table 2
A reference set of physical parameters associated with the calculation of the drainage flux. Note that the parameter E has a large possible range, between 0.65 Pa m and 34 Pa m (Zhu and Chauhan, 2005a,b). Further details are also in the text.

Parameter	Value used
Length Of canaliculi	1.2×10^{-2} m
Radius of canaliculi	2.5×10^{-4} m
Pressure difference between lacrimal sac and canaliculi	400 Pa
Elasticity of canaliculi × Thickness of canaliculi, E	2.9 Pa m

The parameter E is the product of the elastic modulus and thickness of the canaliculi walls, and there is a substantial possible range of this parameter, from 0.65 Pa m to 34 Pa m (Zhu and Chauhan, 2005a,b). Ultimately it is suggested that $E = 2.6$ Pa m yields the most appropriate fit of empirical observations of drainage for the healthy eye; we choose a slightly different value, $E = 2.9$ Pa m. This ensures that the drainage flux for our reference parameters is such that 23% of the total volume, taken to be 7e-9 m^3 as above, drains per minute. This is in the range of percentage tear turnover rates of the normal eye (Goebbels et al., 1992), and other studies (Tomlinson and Khanal, 2005). However it is also higher than a number of other reported measurements of tear turnover in a recent review (Tomlinson and Khanal, 2005); as we will see below we are constrained to consider the larger values of drainage flux reported in the literature.

2.1.1.7. Evaporation rate. While the spreading tear film lipid layer stabilises in the normal subject within the first second of the interblink period, leading to potential differences between evaporation at the start and finish of the interblink, here we simply require an average value, as typically recorded in clinical measurements. Because evaporation varies markedly in dry eye we consider a range of evaporation rates in the simulations below.

However, considering the representative evaporation rate for the normal eye within our model, while taking into account empirical restrictions on the drainage flux, highlights a necessary constraint. Assuming the system behaviour is identical from one blink to the next, as observed below once initial transients have decayed away, a global balance of fluid volume and solute in the interblink shows that

$$\begin{aligned}[\text{Flux from lacrimal gland}] &= \text{Evaporation rate} \times \text{Surface area} \\ &\quad + \frac{\text{Drainage time}}{\text{Interblink time}} \times \text{Drainage flux} \\ &= \frac{\text{Drainage time}}{\text{Interblink time}} \times \text{Drainage flux} \\ &\quad \times \frac{<\text{Meniscus concentration}>}{\text{Isotonic concentration}}\end{aligned}$$

where <Meniscus Concentration> is the integral mean of the meniscus concentration during the drainage part of the interblink. Thus, one immediately has that

$$\frac{<\text{Meniscus concentration}>}{302\ \text{Osm m}^{-3}} = \left(1+\frac{\text{Evaporation rate}\times\text{Exposed surface area}}{\text{Drainage time}\ \times \text{Drainage flux/Interblink time}}\right).$$

The meniscus concentration of normal eyes is observed to be bounded above by 313 Osm m^{-3} in major studies to date (Tomlinson and Khanal, 2005). In addition, in our simulations below we see that the variation in the meniscus concentration during the interblink given the parameters of Table 1 is very small. Thus the above integral mean of the meniscus concentration is the same (to within a fraction of a percent) as any legitimate measurement of the meniscus concentration. Hence, on the additional assumption that potential variables such as the ambient humidity and airflow do not differ significantly among reported measurements, the evaporation rate for the normal eye has a strict upper bound:

$$\begin{aligned}0.0364 &= \frac{313\ \text{Osm m}^{-3}}{302\ \text{Osm m}^{-3}}-1\\ &\geq \frac{\text{Evaporation rate}\times\ \text{Surface area}}{\dfrac{\text{Drainage time}}{\text{Interblink time}}\times\text{Drainage flux}}\\ &= \frac{\text{Evaporation rate}\times 2.46\text{e-}4}{(1/2)\times 5.37\text{e-}11\ \text{m s}^{-1}}.\end{aligned} \tag{4}$$

For consistency with the parameter values of Table 1, which are representative of the normal eye, and the constraint that the meniscus concentration does not exceed 313 Osm m^{-3}, the evaporation rate must therefore be at most 4.0e-9 m s^{-1}. We use this value. Note that this is close to the mean and comfortably within the range of (4.1 ± 1.4)e-9 m s^{-1} reported in the most recent study by Goto et al. (2003), and among those considered in a comprehensive review (Tomlinson and Khanal, 2005). It is similarly close to results reported by Rolando and Refojo (1983), though lower than the mean values from other studies (Tomlinson and Khanal, 2005). A report by King-Smith et al. (2008) has suggested that evaporation rates typically reported in the literature may be low compared to those occurring in natural conditions, due to systematic errors arising from the use of closed pre-ocular chambers. However, while this should be kept in mind, we note that in the study of Goto et al. (2003), using ventilated chambers, the values reported are in keeping with those used here.

More generally, the above constraint forces the use of parameter values towards the upper end of those reported for the drainage flux, and at the lower end of reported values for the evaporation rate, to ensure that the meniscus concentration is appropriately bounded for our representative parameters.

2.1.1.8. The flux from the lacrimal gland. The flux from the lacrimal gland is fixed by the requirement that the total fluid volume is conserved and is thus given by

$$\begin{aligned}&\text{Flux from the lacrimal gland} =\\ &\quad\text{Evaporation rate}\times(\text{Meniscus surface area}\\ &\qquad\qquad+\text{Tear film surface area})\\ &+(\text{Drainage time/Interblink time})\times\text{Drainage flux}.\end{aligned} \tag{5}$$

For the above reference values we find this is equal to 2.8e-11 $m^3\ s^{-1}$, which is within 50% of the mean of values reported by seven authors, as cited by Tomlinson et al. (2006).

2.1.1.9. The flux from the fornical sac into the meniscus. The volume flux into the meniscus from the fornical sac is anticipated to be positive because of the negative hydrostatic pressure within the meniscus (the thirsty meniscus effect) (McDonald and Brubaker, 1971). One can estimate an upper bound from the observation that a small drop of fluorescein placed about 1e-2 m under the lower eyelid takes a mean time of 230 s to appear in the tear film (MacDonald and Maurice, 1991). Hence, assuming the thickness of the retro-tarsal tear layer is no greater than that of the exposed tear film and with P denoting the perimeter of the eyelid as previously, an estimate for an upper bound of the fornical flux is given by

$$\begin{aligned}\frac{1\text{e-}2\text{ms}^{-1}}{230}P\times\text{Tear film depth}&\sim\frac{1\text{e-}2\times5.4\text{e-}2\times3\text{e-}6}{230}\ \text{m}^3\ \text{s}^{-1}\\ &\sim 7\text{e-}12\ \text{m}^3\ \text{s}^{-1}.\end{aligned}$$

Furthermore, if the fornical sac is assumed to act also as a fluid reservoir, within which lacrimal fluid accumulates during the interblink, then the flux from the fornical sac into the meniscus should be much lower than the lacrimal flux. Assuming the latter in the first instance, we simply take the flux form the fornical sac to be a small fraction, 1/6, of the lacrimal flux, which gives 4.7e-12 $m^3\ s^{-1}$. We fix the volume flux into the meniscus as this ratio of the lacrimal flux unless otherwise stated, though we do explicitly consider the variation of this parameter given difficulties in its estimation.

2.1.1.10. The flux from the tear film into the meniscus. We require the mean value of the volume flux for the flow from the tear film into the meniscus during the interblink. It is predominantly driven by capillary forces, and is positive but small compared to the scales set by the meniscus volume and the interblink time. The positivity arises because of the pressure gradients induced by the meniscus curvature via the balance of stresses on the tear–air interface. Its relatively small value is because the pressure gradients act to thin the meniscus-tear film interface essentially decoupling the two compartments (McDonald and Brubaker, 1971). In clinical terms, this corresponds to the formation of the "black line", a dark line of reduced fluorescence at the fluorescein-stained tear film/meniscus junction.

To estimate the flux we note reports suggesting that the meniscus height, h_0, increases by about 10–11% during the interblink (Johnson and Murphy, 2006). We have from the above a relationship between the meniscus volume and the meniscus height; thus one can deduce that a 10–11% increase in the meniscus height for our reference values induces an increase of 15–17% in the meniscus volume. Noting that the flux from the fornical sac above is too small to induce a significant change in the meniscus volume during the interblink, we simply estimate the flux to be

$$\begin{aligned}[\text{Flux from tear film to meniscus}]&\sim\frac{1}{6}\frac{\text{Meniscus volume}}{\text{Interblink time}}\\ &=\frac{1}{6}\frac{1.34\times10^{-9}}{4}=5.58\times10^{-11}\ \text{m}^3\ \text{s}^{-1}\end{aligned}$$

in the reference table of parameters. To investigate model sensitivity to parameters that are difficult to estimate, we additionally consider reducing this flux by an order of magnitude in our studies. Extensively increasing the flux is not considered since then it is predicted that the ocular surface dries out even under healthy eye conditions (which additionally requires the neglect of black line formation and the resultant decoupling of the meniscus and tear film fluid compartments).

2.1.1.11. Initial conditions. The initial conditions, at the start of the first blink, are denoted by

$$\begin{aligned}&V_m(0)=V_m^0,\quad V_{tf}(0)=V_{tf}^0,\quad V_f(0)=V_f^0,\\ &Q_m(0)=Q_m^0,\quad Q_{tf}(0)=Q_{tf}^0,\quad Q_f(0)=Q_f^0.\end{aligned} \tag{6}$$

The values of V_m^0, V_{tf}^0, V_f^0 can be estimated, as discussed above, and are listed in Table 1. The initial solute values have to be assigned, which we do by assuming isotonicity. This is reasonable for the fornical sac concentration given that the lacrimal gland secretions are isotonic. We also briefly consider variation in Q_m^0, Q_{tf}^0 below to show the model is insensitive to the details of these parameter choices.

2.1.2. Parameter variations

We consider the variation of the meniscus radius of curvature, as a surrogate for lacrimal gland function, since lacrimal deficiency is a major cause of dry eye. We also investigate the variation of the evaporation rate in detail, as inadequacies of the tear lipid layer are a major cause of dry eye via enhanced evaporation, typically resulting from meibomian gland disease (MGD). Similarly, we consider a range of interblink times, as increased blinking can be stimulated by the effects of dry eye (Nakamori et al., 1997).

We additionally analyse variation in the flux parameters which are difficult to estimate, namely the flux from the tear film into the meniscus and the flux from the fornical sac into the meniscus. We reduce both by an order of magnitude in our simulations; however consistency restrictions entail that the flux from the tear film into the meniscus cannot be increased by an order of magnitude as substantial increases will entail the tear film is completely depleted within the interblink even for the healthy eye. Thus we only consider increases for the flux into the meniscus from the fornical sac, which corresponds to a scenario where the fornical sac no longer serves as an extensive reservoir of lacrimal gland secretions during the interblink.

2.2. The model for the blink

2.2.1. Model motivation and explanation

First of all we consider the compartment volumes. These will change during the interblink in general and will be reset to their initial values during the completion of a blink.

We proceed to consider solute levels within the compartments. Scintigraphy has been used to track the movement of 0.5 μl of a radioactive tracer in human subjects (Fraunfelder, 1976). This study clearly showed that transfer of tracer from the exposed ocular surface to the fornical fluid is extremely limited. In contrast, tracer did transfer from the fornical fluid onto the exposed ocular surface.

These observations provide detailed information for modelling. For example, an elevated solute concentration upon the exposed ocular surface would not result in a significant transfer of solute to the fornical fluid during a blink. In addition, the fact that there is movement of tracer from the fornices onto the exposed ocular surface entails that solute movement to and from the fornices is not symmetrical; it is thus predominantly flow-induced (advective) in nature even during a blink. Hence below in our mixing model, we take it that the exchange of solutes between the fornical fluid and the exposed ocular surface fluid during the blink is due only to that transfer of fluid between the compartments necessary to reset the compartment volumes. This limitation on mixing is also consistent with observations that small amounts of fluorescein placed under the lower eyelid only start to appear in the tear film on timescales which are about two orders of magnitude longer than the blink–interblink period (MacDonald and Maurice, 1991).

The above-mentioned radiotracer experiment only has the resolution to indicate whether solute transport occurs between different regions of the ocular surface. Thus it does not provide quantitative information about solute transport between the meniscus and tear film during a blink, nor is such information available. Thus, concerning the degree of mixing between these two compartments, at one extreme, one can postulate that during a blink there is perfect mixing between the tear film and the meniscus, plus any fornical fluid that is transferred into the compartments due to these resetting of compartment volumes. This constitutes our maximal mixing model.

At the other extreme, one has that the only solute transport that occurs is due to the movement of fluid among the compartments in order to reset their respective volumes. No additional solute movement, regardless of the fluid dynamics during the blink, is assumed. This constitutes our minimal mixing model. For the minimal mixing model, any transfer of fluid between the fornices and the ocular surface is taken to be between the meniscus and fornical compartments only as these compartments are spatially adjacent and any mixing is deemed to be the minimal consistent with resetting the compartment volumes.

Intermediate levels of mixing are conceived, and hence as a modelling approximation, the extent of mixing is taken to be between the two extremes, except when explicitly investigating the effects of altering the extent of solute mixing during a blink.

2.2.2. Model formulation

2.2.2.1. Compartment volumes. Let V_f^e denote the volume of the fornical sac at the end of the interblink, and let V_f^s denote the volume of the fornical sac at the start of the next interblink, with analogous definitions for $V_m^e, V_m^s, V_{tf}^e, V_{tf}^s, Q_f^e, Q_f^s, Q_m^e, Q_m^s, Q_{tf}^e, Q_{tf}^s$. We take it that

$$V_f^s = V_f^0, \quad V_m^s = V_m^0, \quad V_{tf}^s = V_{tf}^0,$$

for the start of all blinks, where V_f^0, V_m^0, V_{tf}^0 are the initial compartment volumes.

2.2.2.2. Mixing models. To complete our model, we need expressions for Q_f^s, Q_m^s, Q_{tf}^s, that is the solute levels in each compartment at the completion of a blink, or equivalently at the start of the next interblink, in terms of $V_f^e, V_m^e, V_{tf}^e, Q_f^e, Q_m^e, Q_{tf}^e, V_f^s, V_m^s, V_{tf}^s$. These expressions will differ according to the extent of solute mixing between the three compartments. Thus, we firstly derive expressions for Q_f^e, Q_m^e, Q_{tf}^e given the maximal mixing model conceptually described above. Analogous derivations are then presented for the minimal mixing model and then, finally, for the conceived, intermediate, level of mixing.

Case I. (*Maximal mixing*). We initially consider the case where the fornical sac gains fluid during the interblink as a result of continued lacrimal secretion, as this is the typical scenario encountered in the simulations. Since one of the actions of the blink is to reset the volume of the fornical fluid we have that some fluid leaves the fornical sac and enters the compartments of the exposed ocular surface during the blink. Mixing is deemed to be maximal. Thus the fluid from the tear film and the meniscus, plus the fornical fluid entering these compartments is modelled as being thoroughly mixed during the blink. Thus by the end of the blink this fluid has concentration

$$c_0 = \frac{Q_m^e + Q_{tf}^e + \frac{Q_f^e}{V_f^e}\left(V_f^e - V_f^s\right)}{V_m^e + V_{tf}^e + V_f^e - V_f^s}.$$

The denominator is the volume of fluid in the meniscus and tear film at the end of a blink, plus the volume of fluid entering the exposed ocular surface from the fornices; the numerator is the total amount of solute in this fluid. Hence the meniscus and tear film solute levels at the start of the next interblink are, respectively:

$$Q_m^s = c_0 V_m^s, \quad Q_{tf}^s = c_0 V_{tf}^s.$$

The solute level of the fornical fluid is reduced due to fluid of volume $(V_f^e - V_f^s)$, at concentration Q_f^e/V_f^e, leaving the fornices. Hence the new solute level of the fornical fluid compartment is given by

$$Q_f^s = Q_f^e - \left(V_f^e - V_f^s\right)\frac{Q_f^e}{V_f^e} = \frac{Q_f^e}{V_f^e}V_f^s,$$

which is equivalent to the statement that the fornical sac concentration is unchanged. The equations for the case where the fornical sac loses fluid during the interblink can be treated analogously; as mixing is deemed maximal the fluid leaving the ocular surface is, within the modelling, taken to be a well mixed combination of tear film fluid and meniscal fluid.

Case II. (*Minimal mixing*). Again, we initially consider the case where the fornical sac gains fluid during the interblink. Thus, due to resetting the volume of the fornical fluid, some fluid leaves the fornical sac and, as previously, the new solute level in the fornical sac is given by

$$Q_f^s = \frac{Q_f^e}{V_f^e}V_f^s.$$

As mentioned, it is taken that no fluid moves between non-adjacent compartments since mixing is taken to be the minimal consistent with the necessary fluid rearrangements to reset the compartment volumes. Thus, the fluid leaving the fornices is considered to enter only the meniscus compartment. Meniscus fluid is also required to replenish the tear film compartment, as the latter has been depleted, for example by evaporation, during the interblink. Formulating this conceptual model of minimal mixing in a quantitative manner, we have that a volume $(V_{tf}^s - V_{tf}^e)$ of fluid, at concentration Q_m^e/V_m^e, flows into the tear film compartment from the meniscus during the blink giving the solute level in the tear film at the completion of the blink as

$$Q_{tf}^s = Q_{tf}^e + \left(V_{tf}^s - V_{tf}^e\right)\frac{Q_m^e}{V_m^e}.$$

In addition to a volume $(V_{tf}^s - V_{tf}^e)$ of fluid, at concentration Q_m^e/V_m^e, leaving the meniscus compartment, we have a volume $(V_f^s - V_f^e)$ of fluid, at concentration Q_f^e/V_f^e, flows into the meniscus. Thus at the completion of the blink the solute level in the meniscus is given by

$$Q_m^s = Q_m^e - \left(V_{tf}^s - V_{tf}^e\right)\frac{Q_m^e}{V_m^e} + \left(V_f^s - V_f^e\right)\frac{Q_f^e}{V_f^e}.$$

Once more, the case where the fornical sac loses fluid during the interblink can be treated analogously noting that the fornices are taken to be replenished by meniscal fluid only, again by the assumption of minimal mixing.

Case III. (*Intermediate mixing*). The difference between case I and case II is the extent of the mixing. One can model an intermediate level of mixing, between the maximal and minimal cases, by

$$\begin{aligned}
Q_m^s &= Q_m^e + \lambda\left(Q_m^{MaxMix} - Q_m^e\right) + (1-\lambda)\left(Q_m^{MinMix} - Q_m^e\right)\\
Q_f^s &= Q_f^e + \lambda\left(Q_f^{MaxMix} - Q_f^e\right) + (1-\lambda)\left(Q_f^{MinMix} - Q_f^e\right)\\
Q_{tf}^s &= Q_{tf}^e + \lambda\left(Q_{tf}^{MaxMix} - Q_{tf}^e\right) + (1-\lambda)\left(Q_{tf}^{MinMix} - Q_{tf}^e\right).
\end{aligned}$$

Here λ takes values between zero and unity, Q_m^{MaxMix} is the meniscus solute level at the start of the next interblink, according to the above maximal mixing model, while Q_m^{MinMix} is the meniscus solute level at the start of the next interblink, according to the above minimal mixing model. Similarly for

$$Q_f^{MaxMix}, Q_f^{MinMix}, Q_{tf}^{MaxMix}, Q_{tf}^{MinMix}.$$

Thus, $\lambda = 0$ gives minimal mixing and $\lambda = 1$ gives maximal mixing. Results are typically presented below for $\lambda = 0.5$.

2.3. Numerical solution

All parameters are pre-assigned and constant. The ordinary differential equations in the interblink are solved, followed by the rearrangements of compartment volume and solute levels described in Section (2.2) to give the dynamical behaviour from the start of one blink cycle to the next. This is iterated until the dynamical behaviour is identical from one blink cycle to the next; typically 1000 blinks are more than sufficient. This yields the large time asymptote, and the predicted behaviour of the eye once initial transients have decayed; the model predictions are based upon this large time asymptote.

3. Data analysis

3.1. Results for reference parameters, plus the variation of flux parameters

In the following we present results for the parameters in Table 1, which represent a typical healthy eye.

The long time results for these parameter values are given by solid lines in both Figs. 3 and 4. In Fig. 3, the dotted curves correspond to reducing the flux from the tear film into the meniscus by an order of magnitude. In contrast, in Fig. 4, the dotted curves correspond to increasing the flux from the fornical sac into the meniscus by a factor of five while the dashed lines correspond to decreasing this flux by an order of magnitude. When the dashed or dotted plot cannot be seen it is not discernable from the reference parameter results. Note that the slow variations in these plots correspond to model behaviour during the interblink, while the fast variation corresponds to the blink.

Results with different initial choices for the solute levels Q_m^0, Q_{tf}^0, within 10% of the amounts required for isotonicity, reproduce the above plots at large time to at least seven significant figure accuracy; thus the large time asymptote is insensitive to the choice of these initial conditions.

These preliminary results highlight that during the interblink, the tear film concentrations and meniscus concentrations, for the reference parameters, representing a “healthy” eye, are not extensively different though the tear film concentration is greater. In particular, the temporal averages of these quantities differ by at most four Osmoles per cubic metre, a relative difference of less than 1.5%.

Finally, one can observe that these preliminary predictions for concentration levels in the healthy eye are robust to the flux parameters which are difficult to estimate, namely the flux from the fornical sac and the flux from the tears into the meniscus. Analogous comments hold for the level of mixing (results not shown).

3.2. Results for variation in the evaporation rate, the meniscus radius of curvature and the interblink time

3.2.1. Explanation of figures

We now systematically vary both the evaporation rate, and the meniscus radius of curvature for specific values of the interblink time. Of interest firstly are the predictions for the difference between the tear film concentration and the meniscus concentration as these highlight whether meniscus concentration is a useful indicator of ocular surface damage. Predictions for the lacrimal flux are also presented as they indicate regions of parameter space that are inaccessible to an aqueous-deficient dry eye.

For each value of the evaporation rate and the meniscus radius of curvature considered, our simulations generate a value for the tear film concentration and the meniscus concentration at the end of the interblink, once the solution has reached its long time asymptote. They also generate a value for the lacrimal flux. We are

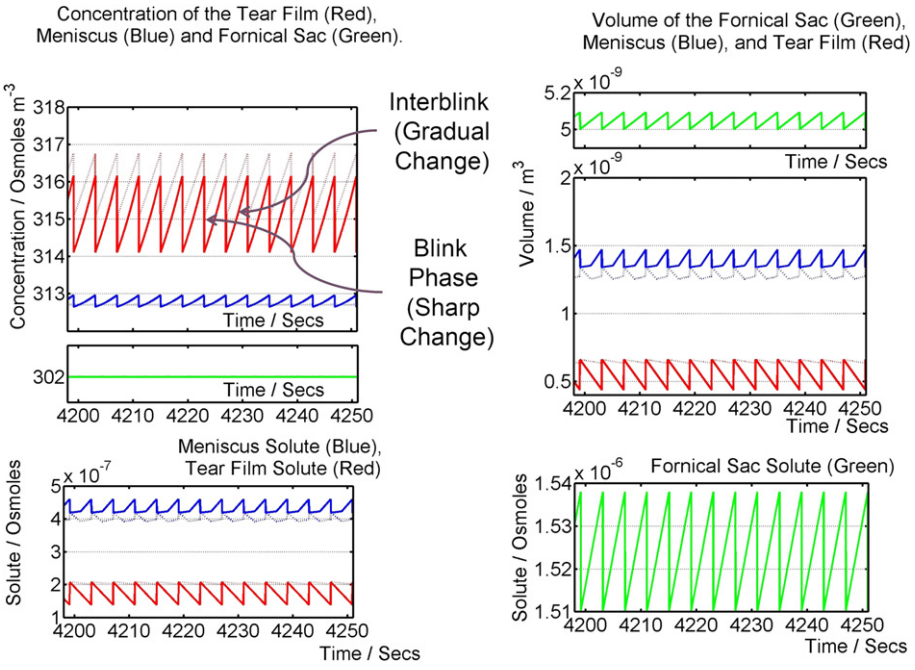

Fig. 3. The large time asymptotes of plots of concentrations, volumes and solute amounts, as functions of time, for 50 s with the reference parameters stipulated in Table 1 and hybrid mixing ($\lambda = 0.5$). The time axis starts at approximately 4200 s, which is longer than 1000 blinks to ensure the system has reached its large time asymptotic behaviour. Results on reducing the flux from the tear film to the meniscus by an order of magnitude are also presented (dotted curves). In this figure, and all subsequent figures, all results are expressed in SI units.

particularly interested in conditions for hyperosmolarity within the ocular surface fluid and especially the tear film; hence meniscus osmolarity is, by far, the most relevant empirical measure as it should be at least correlated with the tear film osmolarity. Thus plotting in terms of meniscus concentration and evaporation rate assists our analysis below, and hence we eliminate the meniscus radius of curvature in favour of the meniscus concentration.

For the parameters of Table 1 and half mixing, Fig. 5 is thus generated by plotting (i) the lacrimal flux and (ii) the difference between the tear film and meniscus concentrations, as functions of meniscus concentration and evaporation rate. For example in plot 5A the value of the lacrimal flux can be determined by comparing the colour plotted at each value of the meniscus osmolarity and evaporation rate with the colour-bar on the right of the plot. Similarly for

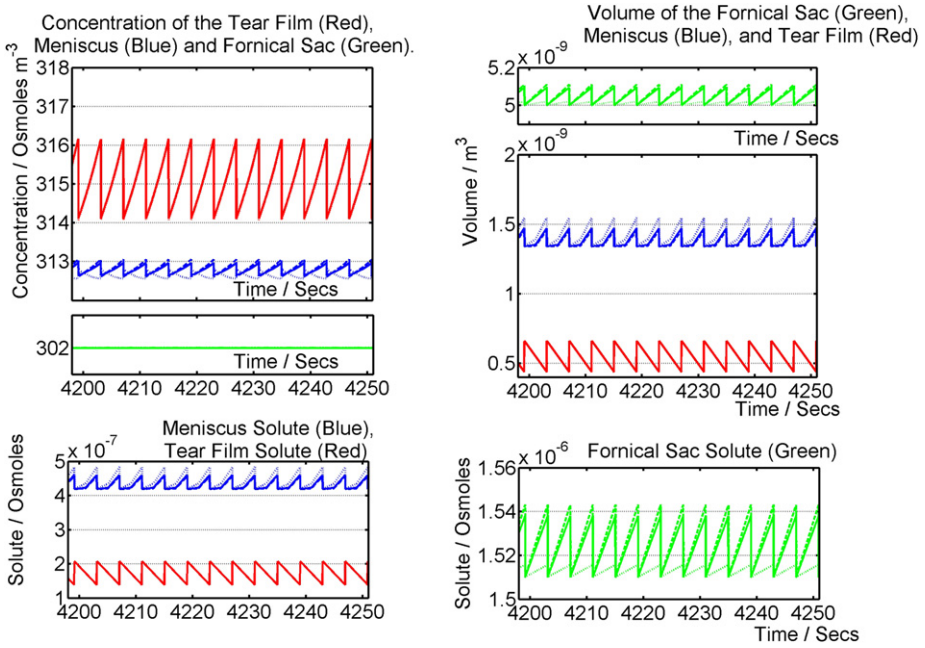

Fig. 4. The large time asymptotes of plots of concentrations, volumes and solute amounts, as functions of time, for 50 s for increasing the flux from the fornical sac into the meniscus by a factor of five (dotted curves) and decreasing this flux by an order of magnitude (dashed curves). Again there is half mixing ($\lambda = 0.5$). The results for the parameters of Table 1 are also given for comparison (solid curves).

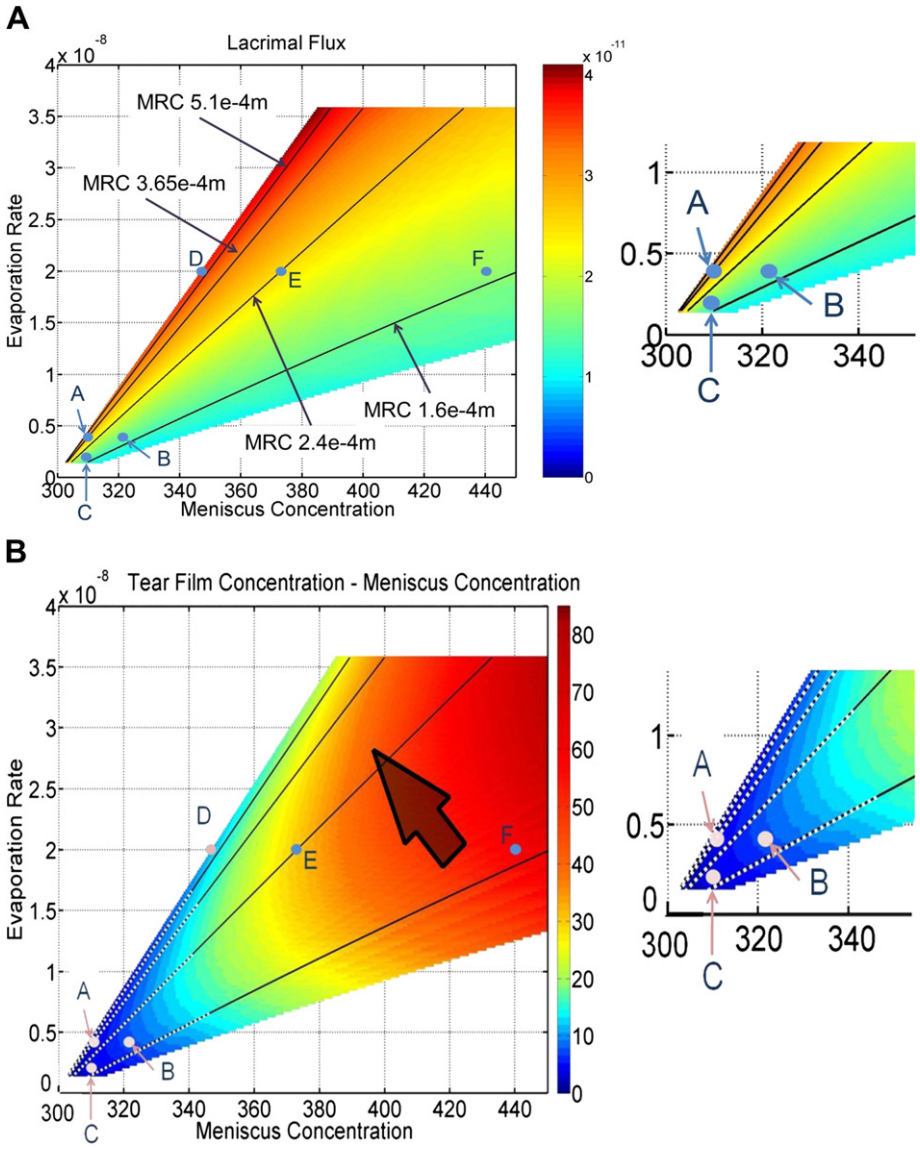

Fig. 5. The upper plot, A, gives the lacrimal flux as a function of the meniscus concentration and the evaporation rate for the reference parameters and half mixing ($\lambda = 0.5$); the inset on the right gives a blow up for a meniscus concentration in the range of 300–355 SI units. The analogous lower plot, B, depicts the difference between the tear film concentration and meniscus concentration. The large arrow in B points from a region of lower meniscus radius of curvature (and lacrimal flux) to a region of higher meniscus radius of curvature (and lacrimal flux). In these and later figures the black diagonal lines (with white dash to aid visualisation) represent a constant value of the meniscus radius of curvature and increase from right to left, taking the respective values 1.6e-4 m, 2.4e-4 m, 3.65e-4 m and 5.1e-4 m, as indicated in A above. See text for further details and for a discussion of the points A–F. Key: MRC, meniscus radius of curvature.

the difference between the tear film and meniscus osmolarities in plot 5B. Note that in these plots, we only consider meniscus concentration values up to 450 Osm m^{-3} where the tear film concentration typically exceeds 500 Osm m^{-3}. Analogous plots, for differing parameter values and levels of mixing, are presented in Figs. 7–10.

The range of the meniscus radii considered is between 1.4e-4 m and 6.6e-4 m; the lower bound is slightly below the minimum observed even in severe dry eye and the upper bound is two standard deviations in excess of the observed mean for the healthy eye (Yokoi et al., 1999, 2004). The black diagonal lines in Figs. 5 and 7–10 refer to contours of constant meniscus radius of curvature. From left to right the meniscus radius of curvature is respectively equal to 5.1e-4 m, 3.65e-4 m, 2.4e-4 m, and 1.6e-4 m. In decreasing order, these values are one standard deviation in excess of the mean for normal eyes, the mean for the normal eye, the mean in dry eye and the smallest value typically observed in dry eye (Yokoi et al., 1999, 2004). In these figures white, unfilled, areas to the upper left correspond to meniscus radii which are higher than commonly observed; analogous areas to the lower right correspond to regions of parameter space where the meniscus radius of curvature is smaller than clinically observed. The model frequently breaks down in the latter of these regions due to insufficient fluid volume to support both a tear film and meniscus.

In addition, in Fig. 6, we present tear film concentrations and meniscus radii of curvature as the lacrimal flux and the interblink time are varied, for two fixed evaporation rates, the lower rate corresponding to a healthy eye, the higher one typifying evaporative dry eye (Tomlinson et al., 2006; Goto et al., 2003).

While we will refer to quantitative details to illustrate trends, it is the qualitative behaviour of the model that is important and the basis for modelling predictions. Unless stated otherwise, these trends and the associated modelling predictions are also true for

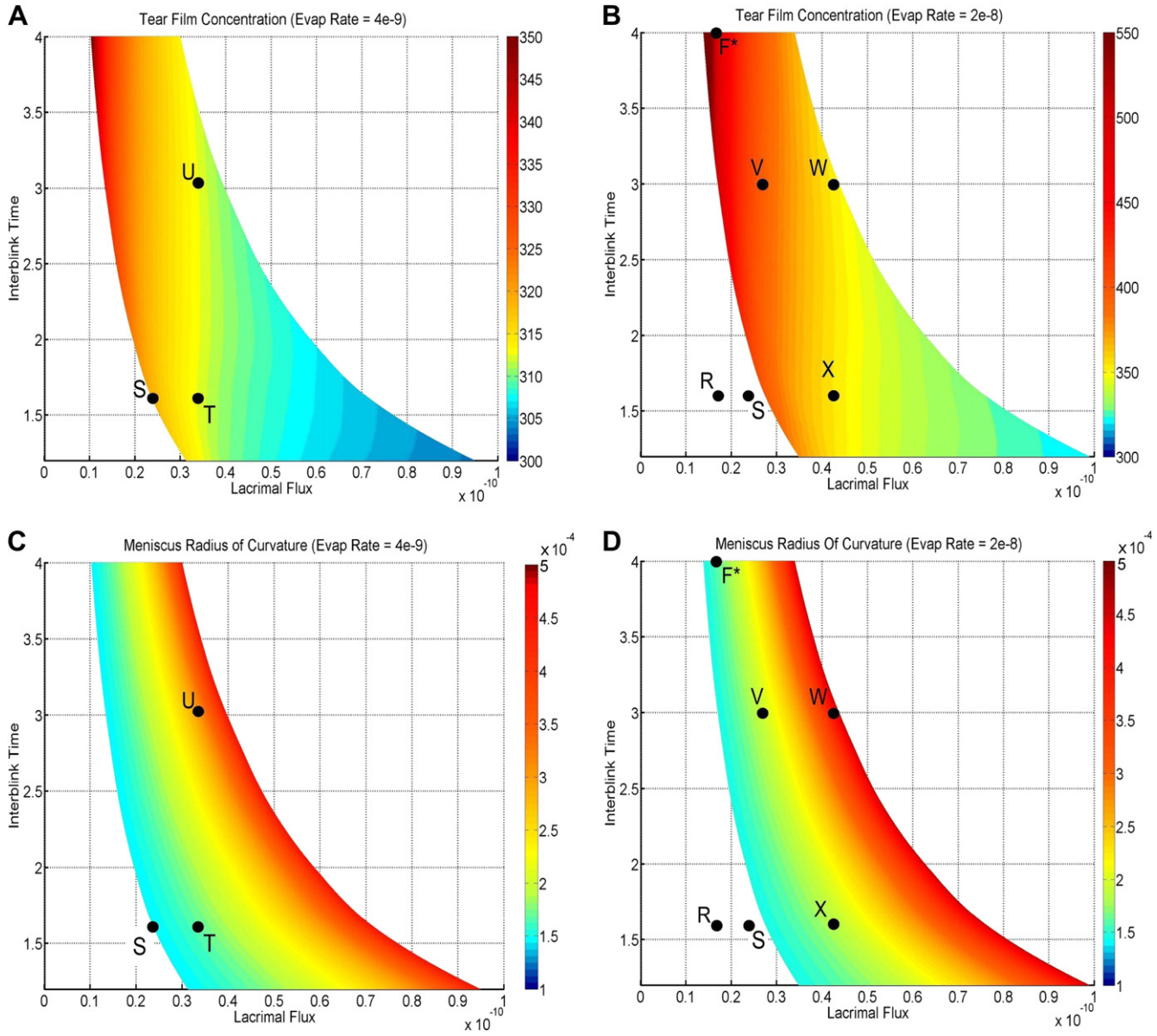

Fig. 6. The upper left plot is A, which depicts the tear film concentration for the representative healthy eye evaporation rate (4.0e-9 m s^{-1}) as the lacrimal flux, in units of m^3 s^{-1}, is varied along the horizontal axis and the interblink time, in seconds, is varied along the vertical axis. Analogous results, but now with an evaporation rate of 2.0e-8 m s^{-1}, typifying evaporative dry eye, are given in B, the upper right hand graph. The corresponding meniscus radii of curvature are given in the lower row, in C,D for the two evaporation rates. One should note the difference in colour scales between the two upper plots. The points F^*, R–X are used to illustrate model predictions in the text.

different levels of mixing and when parameters which are difficult to estimate, such as the flux from the fornical sac, are changed. Thus the following discussion is not sensitive to the difficulties inherent in parameter estimation as detailed further in Section (3.2.4) below.

3.2.2. The healthy eye

Consider Fig. 5A,B. Note that normal, healthy eye parameters are in the lower left of these plots. The evaporation rate of Table 1, namely 4e-9 m s^{-1}, and a meniscus radius of curvature of 3.65e-4 m correspond to point A in both plots; one can read off from the upper plot that the lacrimal flux is approximately 2.8e-11 m^3 s^{-1} and the meniscus concentration is approximately 313 Osm m^{-3}. The difference between the tear film concentration and the meniscus concentration can be determined from point A in Fig. 5B and is predicted to be small. Explicit inspection of the model results (not shown) shows that this difference is less than 1.5% compared to the absolute values of these concentrations. It is also very small compared to the possible range of this difference across parameter space, by inspection of the colour bar in Fig. 5B.

3.2.3. The dry eye

Dry eye often, but not always, stimulates an increased blink frequency (Nakamori et al., 1997). Thus we compare results of the normal eye interblink time of 4.0 s with a typical dry eye interblink time of 1.6 s (Tsubota et al., 1996; Tsubota, 1998), as given in Fig. 7, and we investigate a range of interblink durations in Fig. 6. One should also be alert to the fact that the meniscus radius of curvature typically reduces in ADDE and certainly does not increase (Yokoi et al., 2004); this is less certain for EDE where measurements have not been made.

3.2.3.1. Aqueous-deficient dry eye (ADDE). Consider an aqueous-deficient dry eye with an evaporation rate at the nominal healthy

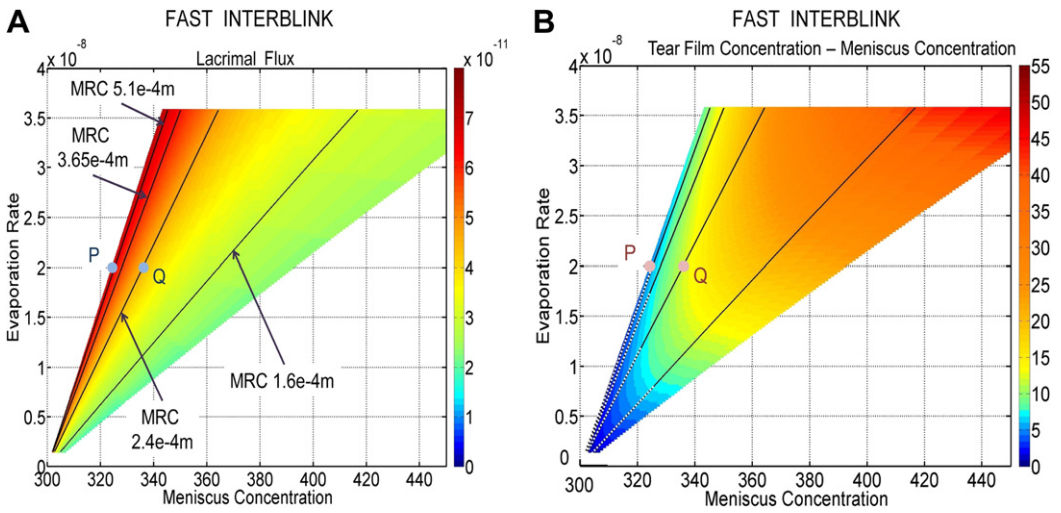

Fig. 7. On the left, constituting A, the lacrimal flux is given as a function of the meniscus concentration and the evaporation rate for the reference parameters with half mixing ($\lambda = 0.5$), and a fast interblink time of 1.6 s. The drainage flux is thus active throughout the interblink. The analogous plot on the right, B, gives the difference between the tear film concentration and meniscus concentration. In the above, and other figures, the black diagonal lines (with white dash to aid visualisation if required) represent a constant value of the meniscus radius of curvature and, from left to right respectively, correspond to the values 5.1e-4 m, 3.65e-4 m, 2.4e-4 m, and 1.6e-4 m, as arrowed. See text for further details and for a discussion of the points P, Q. Key: MRC, meniscus radius of curvature.

level of 4e-9 m s^{-1}. For definiteness, suppose the lacrimal gland can support at most a flux of no greater than 1.75e-11 m^3 s^{-1}, that is 0.0175 μl s^{-1}. This corresponds to point B in the plot of Fig. 5A. One can determine the corresponding meniscus concentration; it is approximately 323 SI units. This allows one to determine the location of point B in Fig. 5B and thus the difference between the tear film and meniscus concentration. One can immediately deduce that it is still relatively small. Explicit inspection of the model results (not shown) shows that it is approximately double that found in the normal eye. One can also determine that there is a substantial reduction in the meniscus radius of curvature as moving from point A to point B requires crossing contours of constant meniscus radius of curvature in a decreasing direction.

Such observations illustrate the general prediction that, as expected, decreasing the lacrimal flux, holding everything else fixed, leads to higher meniscus concentrations and lower meniscus radii, and hence worsening dry eye. Tear film breakup ultimately ensues with further lacrimal flux reductions which move the system further and further right, past the point B. This eventually brings the eye outside the region of parameter space with observed meniscus radii of curvature. Here, either the predictions of meniscus radii are extremely low or, more typically, the model breaks down as it does not predict a stable meniscus and tear film, which is indicative of tear film breakup.

The consequence of an increase in the osmolarity at the ocular surface is an increase in reflex blink rate through stimulation of corneal nerve terminals and the operation of the Lacrimal Functional Unit. If we apply the model to this possibility and, as noted, apply a restriction on the maximal lacrimal response then we find that the highest frequency of blink rate compatible with the lowest observed meniscus radius of curvature is restricted. This can be deduced by inspection of Fig. 7A, which concerns an interblink time of 1.6 s, by noting there is no solution with an observed meniscus radius of curvature when the lacrimal flux is bounded above by 1.75e-11 m^3 s^{-1}. This is confirmed and reinforced by Fig. 6A, which gives tear film concentration when the lacrimal flux and interblink time are varied for the nominal healthy eye evaporation rate of 4e-9 m s^{-1}. In particular, point S in Fig. 6A corresponds to the lowest lacrimal flux consistent with our parameter values (2.4e-11 m^3 s^{-1}, i.e. 0.024 μl s^{-1}), while point T gives the lacrimal flux required for a meniscus radius of curvature at the lower bound of the clinically observed range. One can also immediately see by comparing points T and U in Fig. 6A that for a fixed lacrimal flux, as anticipated in ADDE with the lacrimal gland at maximal capacity, the tear film concentration is relatively insensitive to changes in the interblink time.

Finally, note from Fig. 5A,B that a reduced evaporation rate *can* significantly reverse the effects of a deficient (but non-zero) lacrimal gland flux; this can be seen by starting at point B and moving to point C, that is reducing the evaporation while keeping the lacrimal flux fixed. Note that the meniscus concentration, the tear film concentration and the difference between these all decrease.

3.2.3.2. Evaporative dry eye (EDE). Consider increasing the evaporation rate for an otherwise healthy eye. For definiteness, take the evaporation rate to be 2.0e-8 m s^{-1} which is typical of evaporative dry eye values (Tomlinson and Khanal, 2005). It is, however, a factor of eight less than the evaporation rate of pure water at a typical (30%) value of humidity (McCulley and Shine, 2000) and much less than the evaporation rates of pure water in hot, dry and windy conditions.

For the interblink time of 4.0 s implicit in Fig. 5A,B there is no stable tear film state, regardless of lacrimal function, that can maintain the meniscus concentration at healthy levels, at least given observed upper bounds on the meniscus radius of curvature.

We proceed to consider the ocular surface's response as the evaporation rate changes slowly from the nominal healthy value of 4.0e-9 m s^{-1} to the above-mentioned pathological value of 2e-8 m s^{-1}. This represents the evolution of evaporative dry eye over time assuming the blink rate is fixed. If the meniscus concentration was held fixed, one would move vertically upwards from point A in Fig. 5A,B resulting in an increase in both the lacrimal flux and the meniscus radius of curvature. However, in the real world situation and as suggested above, the increase in evaporation rate would be accompanied by an increase in the meniscus concentration. Thus the ocular state will move from the point A in an oblique direction towards the upper right in Fig. 5A,B as the evaporation increases.

The final point depends on the extent to which the lacrimal flux can be upregulated to compensate the increase in evaporation rate. For example, if a maximal lacrimal flux of 3.7e-11 m^3 s^{-1} is sustainable, which is the lacrimal flux at point D in Fig. 5A,B, the ocular state will evolve to this point, assuming the blink rate is fixed; here, the

meniscus and tear film concentrations are 347 Osm m^{-3} and 360 Osm m^{-3} respectively. However note that the meniscus radius of curvature at D is 6.6e-4 m, which is outside the observed range currently reported for any form of dry eye, though we are aware that studies of EDE at all stages of development have not yet been conducted.

Furthermore, if only smaller sustainable lacrimal fluxes are possible the ocular state will eventually evolve to a point to the right of D. For example, with a maximal sustainable lacrimal flux of 2.6e-11 m^3 s^{-1}, which is approximately the normal value, the ocular state is predicted to evolve from point A to point E in Fig. 5A,B as the evaporation rate is increased. The meniscus radius of curvature at this endpoint, E, is 2.4e-4 m which is much less than at point D and corresponds to the mean of observed dry eye values currently reported in the literature; the meniscus and tear film concentrations are 372 Osm m^{-3} and 401 Osm m^{-3} respectively.

We continue to consider evaporative dry eye but now with a typical dry eye interblink of 1.6 s, corresponding to Fig. 7A,B. For robust lacrimal function, capable of producing a sustainable flux of 7e-11 m^3 s^{-1}, we see the ocular state will evolve to the endpoint P, where the meniscus and tear film concentrations are 324 Osm m^{-3} and 329 Osm m^{-3} respectively. However, this is again accompanied by an increase in the meniscus radius of curvature to a value which is not currently observed for any form of dry eye. For the observed mean dry eye meniscus radius of curvature, namely 2.4e-4 m (Yokoi et al., 2004), the ocular state reaches the endpoint Q where the meniscus concentration is about 335 Osm m^{-3} and the tear film concentration is about 346 Osm m^{-3}, which is lower than at points D, E in Fig. 5B; the lacrimal flux demand is 4.6e-11 m^3 s^{-1}, which is larger than the lacrimal flux estimated in the healthy eye.

These trends are illustrated more generally by Fig. 6B,D where the evaporation rate is elevated, at 2.0e-8 m s^{-1}. One can clearly see, by comparing points V and X, that reducing the interblink time and increasing the lacrimal flux reduces the ocular surface concentrations. One can also observe from comparing points V and W that upregulation of the lacrimal flux without a sufficient increase in blink frequency will also result in large meniscus radii of curvature, above the observed range.

Finally note that, as expected, continually increasing the evaporation rate without any compensatory mechanisms, i.e. keeping all other parameters fixed, will eventually result in predictions of extremely low meniscus radius of curvature, prior to model break down, implying tear film breakup. This is illustrated by comparing point S in plot 6A with point S in plot 6B. The only difference is the increase in evaporation rate from 4e-9 m s^{-1} in plot 6A to 2e-8 m s^{-1} in plot 6B which pushes the system into the region of parameter space with extremely low meniscus radii of curvature and model break down.

3.2.3.3. Hybrid dry eye. We consider dry eye states that have features of evaporative dry eye and of sub-normal lacrimal gland flux; suppose the evaporation rate is increased, again to 2.0e-8 m s^{-1} with a Lacrimal Functional Unit capable of producing, at most, a lacrimal flux of 1.75e-11 m^3 s^{-1}. Consider, for example, point R in Fig. 6B,D which is in the region of parameter space with either extremely low meniscus radii of curvature or, more typically, model break down, indicating tear film breakup. From this, we immediately see that a tear film with a realistic meniscus radius of curvature cannot form for an interblink time of 1.6 s. In contrast, consider point F in Fig. 5A,B, or equivalently, point F^*, in Fig. 6B,D. This shows that a stable tear film can form given an interblink time of 4.0 s for this lacrimal flux and evaporation rate. However by inspection of Fig. 5A, the meniscus concentration is very large, around 440 Osm m^{-3}, and there is a very high tear film concentration of approximately 500 Osm m^{-3}. In addition, the meniscus radius of curvature is 1.67e-4 m which is just above the smallest observed values. Finally, by considering points W and X in Fig. 6B, we can see that changing the interblink time has no significant effect on osmolarities for a fixed lacrimal flux, as previously observed for aqueous-deficient dry eye at lower evaporation rates.

We now compare the meniscus and tear concentrations in Fig. 5B for both ADDE and EDE. In ADDE, the extent to which these osmolarities can increase is limited. As the maximal lacrimal flux is reduced in ADDE alone, one proceeds from point A to point B in Fig. 5B and then further rightwards. The model does not predict ever increasing osmolarities but instead proceeds to predict meniscus radii lower than observed and subsequently the absence of a stable meniscus and tear film. In contrast, much higher osmolarities are predicted to occur, with the retention of a stable tear film, for either EDE or hybrid pathologies compared to ADDE. This can be explicitly seen by considering the osmolarities along the line passing through the points D, E, F in Fig. 5A,B where the evaporation rate is raised. One can also readily deduce on moving from point D to F in Fig. 5B that the presence of both lacrimal insufficiency and excess evaporation, which typify a hybrid form of severe combined ADDE and EDE, entails that large differences between the tear film concentration and the meniscus concentration accompany the large meniscus osmolarity. This also shows a combination of large meniscus concentration and small meniscus curvature signifies extreme differences between the tear film and meniscus concentrations.

3.2.4. Results for parameter variations

In Figs. 8 and 9 we present analogous results to the above except that we now have maximal mixing rather than half mixing. One can observe that the qualitative trends discussed above are insensitive to this increase in the level of mixing; generally they are robust with respect to the details of the extent of mixing that occurs.

In Fig. 10 we present a simulation for the reference parameters, with half mixing, except that there is a fast interblink of 1.6 s *and* the flux from the fornical sac has been increased by a factor of five. In this scenario the fornical sac is not acting as a reservoir of fluid but, to a good approximation, merely a conduit, efficiently transporting fluid intake from the lacrimal gland into the meniscus. Despite this qualitative difference in the fluid handling properties of the fornical sac, one should note that the qualitative features of these plots are the same as those for the reference parameters. Similarly, the plots produced by reducing the flux from the fornical sac, or reducing the flux from the tear film to the meniscus by an order of magnitude do not induce a qualitative difference (results not shown). There are slight quantitative differences between figures on varying parameter values, the most extreme of which is observed on comparing Figs. 5B and 10B, as highlighted in the caption of the latter. Nonetheless such differences do not prevent the inference that all of the observed trends are not invalidated on altering the fluxes which were difficult to estimate from empirical data.

4. Discussion

In this report we used a mass and solute balance model to address the influence of different lacrimal tear secretory and tear evaporative rates on tear osmolarity, including the differential osmolarity between the meniscus and tear film. In this analysis, changes in meniscus radius of curvature served as a surrogate for changes in lacrimal tear flow. We also considered the potential efficacy of compensatory events such as blinking. To our knowledge, this is the first time that a modelling approach has been applied to the factors which regulate human tear osmolarity.

The model for the selected parameters of Table 1, representative of the normal eye, produces a prediction of meniscus concentration which is within the reported ranges (Tomlinson and Khanal, 2005).

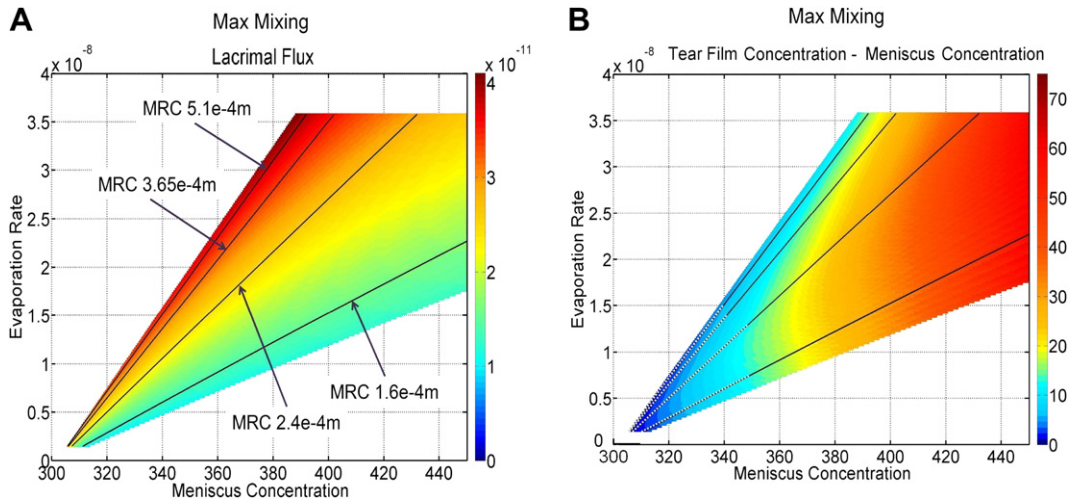

Fig. 8. On the left is A, which depicts the lacrimal flux as a function of the meniscus concentration and the evaporation rate for the reference parameters and maximal mixing ($\lambda = 1.0$). The analogous plot on the right is B, which shows the difference between the tear film concentration and meniscus concentration. Key: MRC, meniscus radius of curvature.

Note however that the constraints of global balance enforce the use of evaporation rates at the lower end of the reported range in the literature and drainage fluxes at the upper end of the reported range. This will require further scrutiny in future models. Given that global balance is one of the few biophysical principles that has to hold for the ocular surface fluid, this also suggests that the simultaneous measurement of multiple parameters in a single eye, with an attempt to balance fluid in and out of the fluid compartments, is likely to refine current measurements.

After considering the normal eye our model proceeds to consider the effect of changing evaporation and tear flow on tear osmolarity in dry eye. The model addresses those dry eye states where the lacrimal apparatus can maintain an intact tear film during the interblink. Assuming that tear film hyperosmolarity contributes to the induction of ocular surface damage in dry eye and to the occurrence of symptoms, surrogates of tear film osmolarity are of considerable interest. Since it is possible to measure meniscus osmolarity in nanolitre samples of tear fluid, it is thus important to know whether the values obtained predict osmolarity levels in the tear film itself. From a conceptual model, we have previously predicted that tear film molarity will be higher than meniscal osmolarity (Bron et al., 2002). The reasons for this difference are, firstly, that the favourable surface area to volume ratio of the meniscus reduces the concentrating effects of evaporation. Secondly in the normal eye, the meniscus rather than the tear film is refreshed during the interblink by near isotonic fluid from the fornical sac.

This expectation has been borne out by the modelling conducted in the present study which predicts that a difference between the tear film and meniscus concentration is always present and positive, but is small under normal conditions compared to the absolute values and possible ranges of these concentrations. Since the concentration difference between the tear and meniscus is small, one immediately has that evaporation during the interblink is not normally expected to lead to an excessive differential between tear and meniscus concentrations. This in turn yields the prediction of an absence of osmotically induced ocular surface damage for the normal eye, while highlighting that attempting to detect differences between tear film and meniscus osmolarities would be unprofitable in the absence of pathology. Such predictions are robust to variations in the parameters that are difficult to estimate as varying these does not alter the qualitative features of the results; similarly for the rest of the discussion below.

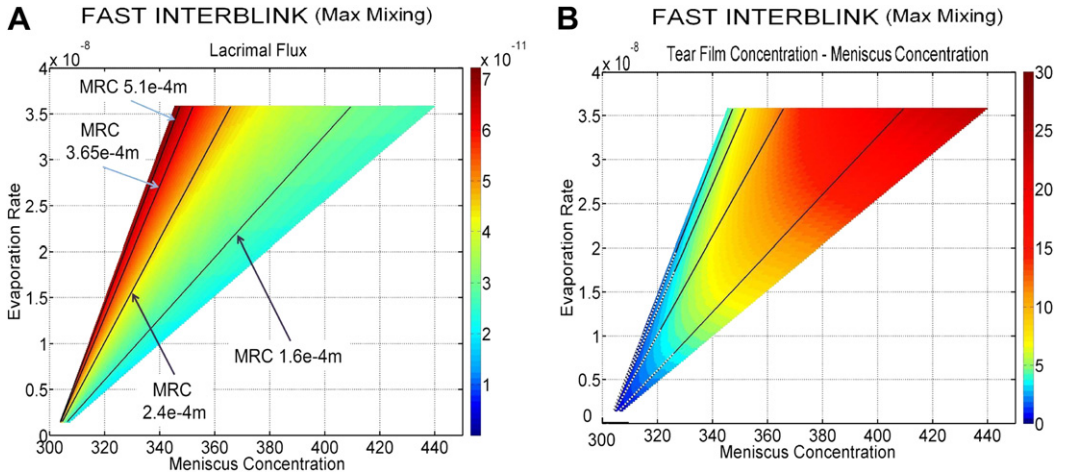

Fig. 9. On the left is A, which depicts the lacrimal flux as a function of the meniscus concentration and the evaporation rate for the reference parameters, except that we have the fast interblink of 1.6 s, the drainage flux is active throughout the blink, and maximal mixing ($\lambda = 1.0$). The analogous plot on the right is B, which shows the difference between the tear film concentration and meniscus concentration. Key: MRC, meniscus radius of curvature.

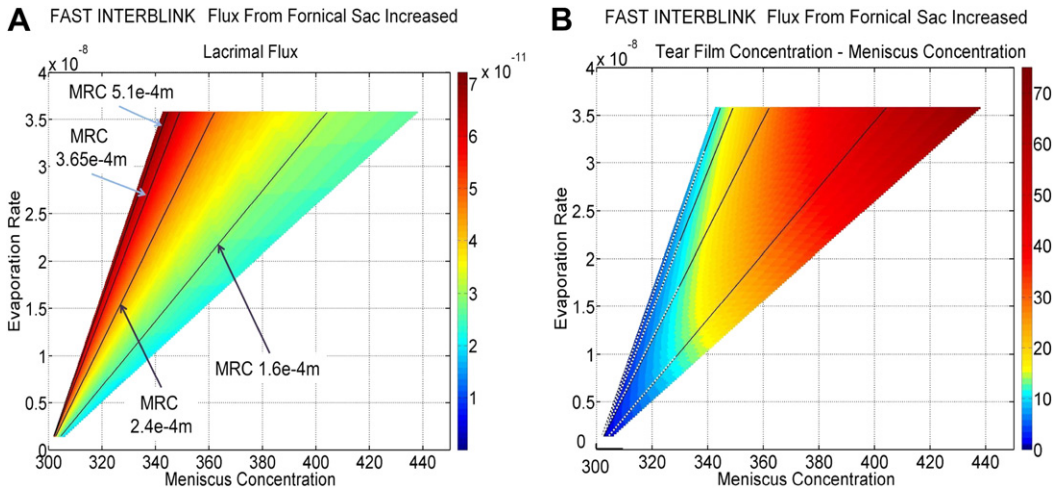

Fig. 10. On the left is A, which depicts the lacrimal flux as a function of the meniscus concentration and the evaporation rate for the reference parameters, except that we have increased the flux from the fornical sac into the meniscus by a factor of five; there is half mixing ($\lambda = 0.5$). The analogous plot on the right is B, which shows the difference between the tear film concentration and meniscus concentration. Note that the plot of the difference between the tear film concentration and the meniscus concentration has a decreased "elbow" compared to Fig. 5B. To observe this compare the yellow contour of B above to the analogous contour in Fig. 5B, and note that it turns much more sharply in the latter. Further details are in the text. Key: MRC, meniscus radius of curvature.

Nonetheless, one can also readily deduce that where ADDE and EDE occur in combination (as is common in Sjögren's Syndrome (Shimazaki et al., 1998)) the difference between the tear film concentration and the meniscus concentration in this severe form of dry eye is large. An inspection of the results presented here also shows that the combination of a high meniscus concentration and a low radius meniscus of curvature, both of which are generally measurable, is indicative of an elevated difference between the two compartments compared to normal. Such observations on the difference between the tear and meniscus concentrations are relevant to understanding how meniscus osmolarity values relate to symptoms and ocular surface damage in a given patient. Due to unknowns, such as the levels of mixing, it would be inappropriate to use modelling to attempt to quantify this relationship in detail at this stage.

We also have the modelling prediction that reductions in evaporation can readily compensate for the effects of aqueous deficiency, providing that the lacrimal gland function is sufficient to maintain a continuous tear film. Such reductions might be achieved in the clinical situation, by a high ambient relative humidity, either environmental (Ousler et al., 2008) or by using conserving spectacles (Tsubota, 1989). Alternatively it can be achieved by a narrowing of the palpebral aperture.

In addition, we have shown that the compensatory mechanism of an increased blink rate, achieved by feedback through the Lacrimal Functional Unit, should be effective in reducing ocular surface concentrations in EDE, but less so in ADDE where lacrimal disease limits the maximal lacrimal gland capacity. The modelling illustrates that a significant increase in the blink rate (and therefore reduction in the interblink time), places a substantial demand on the lacrimal apparatus to maintain meniscus volume and to prevent the eye literally, pumping (i.e. blinking) the tear film dry. Thus a similar increase in blink rate in the two dry eye states may have different implications in terms of compensation.

It is noted in contrast that with the parameters selected, the compensation mechanism of increased lacrimal flux in EDE, in the absence of an increased blink rate, cannot fully compensate for an increased tear osmolarity induced by high evaporation rates given the constraint of the upper limits of observed dry-eye meniscus radius of curvature. However, it is not certain that the literature reflects the highest range of meniscus radius of curvatures which might be encountered in patients with extensive MGD or in EDE states and this area requires further experimental data. At present the model predicts and requires that in EDE, compensation necessitates a concomitant increase in the blink rate.

As expected, we found that either lacrimal deficiency or excess evaporation is sufficient for the induction of dry eye. However, we note that, with the evolution of ADDE and the progressive reduction in lacrimal flux, a point is predicted where tear volume is insufficient to support a stable meniscus and tear film. If EDE, or a hybrid pathology, is examined in the same way, with the anticipation of a progressive rise in the rate of evaporative tear loss, then the condition is able to support a stable meniscus and tear film at much higher hyperosmolar values than in ADDE. Thus, unless in this instance some other factor intervenes to cause earlier tear breakup in EDE (such as goblet cell loss and or a deficiency of membrane-spanning mucins), higher degrees of hyperosmolarity before the advent of tear film breakup, are predicted in chronic, severe EDE or hybrid dry eye, compared with chronic severe ADDE. While the model predicts that hyperosmolarity on approaching breakup is lower in ADDE than EDE, it does become invalid shortly prior to breakup. Past this point and certainly once breakup has occurred, it is anticipated that osmolarity will continue to increase, up to and beyond breakup, both in the residual tear film and particularly within regions of breakup, where the corneal epithelium will be directly exposed.

As mentioned above, the model is only capable of addressing dry eye pathologies where the lacrimal apparatus can maintain an intact film during the interblink. This may be better understood by a consideration of the Ocular Protection Index (OPI) which is the ratio of the Fluorescein Break Up Time (FBUT) to the blink interval. When the blink interval is shorter than the breakup time, the OPI is greater than unity and breakup does not occur during the interblink. This does not however exclude the presence of tear film instability (Goto et al., 2008; Kojima et al., 2004) or high degrees of tear film thinning (Nichols et al., 2005), short of causing tear film breakup. An OPI of less than unity implies breakup during the blink interval.

Begley and colleagues have carried out extensive studies of the relationship between tear film breakup and dry eye (Begley et al., 2006; Liu et al., 2006; Harrison et al., 2008) and have further compared the character and intensity of symptoms associated with tear film breakup with those induced by hyperosmolar solution instilled onto the surface of the eye (Liu et al., 2009). These studies have indicated a threshold for the induction of symptoms at an

osmolarity of 450 Osm m^{-3} (450 mOsm l^{-1}) with 800–900 Osm m^{-3} required to mimic symptoms induced by breakup. This corresponds to the situation in dry eye patients where the OPI is less than one. What is less clear but nonetheless important is whether the levels of hyperosmolarity shown to induce symptoms in such studies can be generated at the ocular surface in dry eye patients with OPI values greater than one. These will occur in patients diagnosed as having dry eye on the basis of a reduced FBUT but whose breakup values are still greater than the interblink duration in that individual.

What is the relevance of the findings of Liu et al. (2009) to the dry eye patients addressed in our model with an OPI of greater than one? The highest levels of tear film molarity generated by our model for typical dry eye evaporation rates is in the region of 500–600 Osm m^{-3} in a hybrid situation of combined ADDE and EDE, e.g. Point F in Fig. 5B. This exceeds the symptom threshold of 450 Osm m^{-3}. In our model such high tear film osmolarities correspond to a meniscus osmolarity of around 440–500 Osm m^{-3}; again consider point F of Fig. 5B for an example. Cited meniscus osmolarities in dry eye have been recorded up to 360 Osm m^{-3} by Gilbard and Farris (1979) but higher levels have been reported by Lee et al. (2000), i.e. 402 Osm m^{-3} three months after PRK and 481 Osm m^{-3} three months after LASIK surgery. However, achieving these extremes in our modelling typically requires the presence of EDE and ADDE in combination within a hybrid dry eye, *plus* some tuning of parameters. For example in Fig. 9B such extremes are not achieved even for hybrid dry eye states; the difference between the dry eye states observed at Point F in Fig. 5B and those in Fig. 9B is that the level of mixing during the blink is substantially higher in the latter.

The fact that the model does not universally predict the concentrations required for symptom thresholds in all dry eye states and typically does not predict osmolarities in the region of 800–900 Osm m^{-3} should not be considered to be in conflict with the report of Liu et al. (2009). Their results describe expectations in dry eye patients with OPI values lower than unity, whereas our predictions relate only to patients in whom the OPI is greater than unity. It remains uncertain whether symptoms due to tear film hyperosmolarity can be generated in the absence of tear film breakup in all dry eye states with an OPI of greater than one. However, we anticipate that our model underestimates the highest tear film molarity which might be achieved in dry eye prior to breakup. In particular, we explicitly consider only an average osmolarity across the whole tear film compartment. As noted by Liu et al. (2009), the fact that tear film breakup occurs at distinct points suggests that, sufficiently close to breakup, there will be local fluctuations in the tear film thickness which would induce hyperosmolarity "hot-spots" with significantly higher concentrations than the average. Another consistent explanatory hypothesis would be that symptoms in patients with an OPI of greater than one have a basis other than or in addition to hyperosmolarity, and which could include friction between the mucous membranes of the lid and globe or the release of inflammatory mediators.

A potential limitation of our compartmental model is that it does not allow us to entertain high lacrimal fluxes which may be conceptually predicted to occur as a compensatory response in EDE. In our model, lacrimal flux monotonically increases with meniscus radius, and thus the latter may be considered as a surrogate for the former. The meniscus radius is constrained by its currently observed upper bound, which may not reflect values present in evaporative dry eye; thus restricting our modelling to currently observed values of the meniscus radius of curvature does limit the lacrimal flux. However, because the contours of constant meniscus curvature approach confluence as the meniscus radius increases, these particular empirically based constraints do not dramatically influence the modelling's current representation of high fluxes.

A critical factor does however emerge in attempting to consider very high lacrimal fluxes. Because of the requirement for global balance, the lacrimal flux cannot exceed the drainage flux. Thus, within the model in the presence of high lacrimal fluxes, exceeding normal levels by a few multiples or more, there is no means to drain the eye sufficiently quickly using the drainage model Zhu and Chauhan (2005a,b). While this previous work has advocated that the current drainage model is valid for the overloaded tear film, the validity of all the implicit assumptions required in the current framework under high flux conditions is unclear. In particular, in the presence of extremely high lacrimal fluxes, both Zhu and Chauhan's (2005b) use of the lubrication theory approximation for the meniscus pressure and our implicit modelling assumption of a uniform meniscus radius are suspect. Thus, further modelling, accompanied by a postulate of extremely high lacrimal fluxes plus a detailed consideration of drainage and spatial variation may predict the possibility of a distinct dry eye phenotype which cannot be considered further here. As mentioned, measurements of the meniscus radius of curvature in the presence of EDE are also likely to be highly informative.

A high lacrimal flux phenotype may additionally be highly relevant for modelling the ocular surface fluid during VDU work, where the blink rate falls substantially to as low as five per minute (Blehm et al., 2005; Nielsen et al., 2008), which extensively increases evaporative loss for an otherwise healthy eye on a transient basis in the absence of other pathology.

5. Summary and future directions

In summary, we have constructed a simple model for the mass and solute balance in the tear film, incorporating extensive empirical data, with conclusions that are insensitive to the difficulties encountered in parameter estimation. The model predictions for the normal eye are consistent with observation and demonstrate a differential between tear film and meniscus concentrations under normal circumstances, the concentration always being higher in the tear film. This differential rises in dry eye, especially in the presence of a hybrid pathology combining aspects of ADDE and EDE. Also of note is the fact that higher osmolarities can be achieved within a stable tear film for EDE or with hybrid pathologies rather than ADDE alone, at least assuming no other factors such as ocular surface abnormalities intervene to cause breakup. The modelling also indicates that the combination of an elevated meniscus concentration and a reduced meniscus radius of curvature is indicative of large differences between the tear film and meniscus concentrations. The influence of compensatory mechanisms has also been explored, revealing that rapid blinking is predicted to reduce ocular surface osmolarities providing the rise in lacrimal demand can be met to prevent the eye pumping the tear film dry. This indicates a differential efficiency of compensatory events according to the cause of dry eye and may be investigated by further empirical studies. Overall we found that no single parameter is a universal surrogate for tear film concentration and its role in ocular surface damage. Finally, the difficulties in parameter estimation suggest that multiple measurements of fluid fluxes for an individual eye, taking mass balance into account, is likely to refine current measurements.

One should note that the use of crude compartments in the current modelling framework is a considerable simplification. Refining the spatial aspects of the ocular surface fluid will allow the exploration of numerous features of the tear film which cannot be considered in the current framework. For example, simply introducing upper and lower fornix and meniscus compartments would allow the investigation of the tear surface osmolarity profiles emerging from extensive partial blinking, where there is incomplete mixing between upper and lower compartments on the exposed ocular surface. Similarly, focussing on the solute levels around an initial tear film breakup will allow the exploration of the

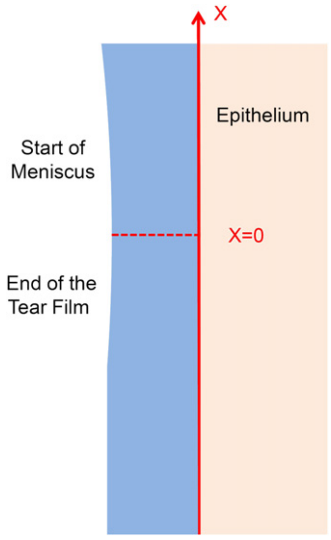

Fig. 11. The figure shows the pre-ocular fluid around the tear-meniscus boundary, illustrating the spatial variable x used in the appendix.

mechanisms generating hyperosmolarity peaks, which is beyond the scope of the current study. Ultimately, an ambitious goal would be to integrate the modelling of solute balance with continuum models of tear film dynamics (Braun and Fitt, 2003; Braun and King-Smith, 2007; Wong et al., 1996), possibly utilising real time, spatially distributed, measurements of tear film height evolution (King-Smith et al., 2006) to assist model construction or validation. Such approaches would allow an integrated exploration of spatially heterogeneous osmolarity within the tear film.

From our investigations it is also apparent that additional modelling and experimental work is necessary to understand whether high lacrimal flux compensation can be present in EDE and for VDU work, and if so, the likely osmolarity profile of such phenotypes. As such prospects highlight, there may be more than the standard aqueous deficient and evaporative phenotypes of dry eye. Indeed a current conceptual model (Bron et al., 2009) has suggested the possibility of hybrid phenotypes emerging from the progression of organic disease, with a functional aqueous tear deficiency being induced by EDE and a functional, increased, evaporative component being added to a primary ADDE. Future empirical studies testing such hypotheses and modelling generalisations exploring and characterising predictions for disease evolution in dry eye are therefore also likely to be fruitful avenues for further research.

Acknowledgements

We are extremely grateful to Professor Caroline Begley for insightful discussions and for making her work available to us (Liu et al., 2009) prior to publication. This publication is based on work supported in part by Award No. KUK-C1-013-04, made by King Abdullah University of Science and Technology (KAUST).

Appendix. On the neglect of diffusion in the interblink

Diffusion, that is the passive movement of solutes down concentration gradients, is neglected in our modelling framework of solute transport in the interblink, which requires justification. We first of all consider the tear-meniscus boundary. Osmolarity is considered to be due to a single molecular species; generalisations to multiple physiological salts can readily be implemented and will not change the conclusions.

The height of the pre-ocular fluid at the boundary of the meniscus and tear compartments is much smaller than the lengthscales of distances along the surface of the eye in both the meniscus and the tear film. It is also much smaller than the distance from the tear-meniscus boundary to the centroid of the cornea. Then, at leading orders in expansions in the aspect ratio, the advection–diffusion equation reduces to its one dimensional form[1]

$$\frac{\partial c}{\partial t} = D\frac{\partial^2 c}{\partial x^2} + U\frac{\partial c}{\partial x},$$

where c is the solute concentration, averaged across the depth of the thin film, and $x = 0$ corresponds to the tear-meniscus boundary, as depicted in Fig. 11. The term $D\partial^2 c/\partial x^2$ corresponds to diffusion, where D is the diffusion coefficient. The term $U\partial c/\partial x$ models the effects of advection, where U is the average across the depth of thin film for the fluid velocity in x-direction, and constant with respect to spatial variables. We simplify our approximation by treating U as constant in time too, which is self-consistent with our modelling framework. With c_m^0 denoting the meniscus concentration at time t_0, the start of the interblink, with $c = c_m^0$ for $x > 0$ at $t = t_0$, and c_{tf}^0 denoting the tear film concentration at time t_0 with $c = c_{tf}^0$ for $x < 0$ at $t = t_0$, one can easily confirm the required solution is

$$c(x,t) = c_m^0 + \left[c_{tf}^0 - c_m^0\right]\frac{2}{\sqrt{\pi}}\int_{\frac{x-Ut}{2\sqrt{D(t-t_0)}}}^{\infty} ds e^{-s^2}. \tag{7}$$

Hence an upper bound on the magnitude of the mean diffusive flux of solute from the tear film compartment to the meniscus boundary is

$$\left|D\frac{1}{T}\int_{t_0}^{t_0+T} dt \left.\frac{\partial c}{\partial x}\right|_{x=Ut}\right| = \left|c_{tf}^0 - c_m^0\right|\frac{1}{T}\int_{t_0}^{t_0+T} dt\sqrt{\frac{D}{\pi(t-t_0)}}$$
$$= 2\sqrt{\frac{D}{\pi T}}\left|c_{tf}^0 - c_m^0\right|.$$

We require that this is much less than the advective flux, Uc_{tf}, where c_{tf} is the concentration in the tear film. A lower bound on U is given by $F/[Pd]$ where F is the flux from the tear film to the meniscus used in the modelling, P is the perimeter of the eyelids and d is the depth of the tear film at the start of the interblink. Thus,

$$1 \gg 2\frac{\left|c_{tf}^0 - c_m^0\right|}{c_{tf}}\frac{Pd}{F}\sqrt{\frac{D}{\pi T}} \tag{8}$$

is sufficient to ensure the effects of diffusion at the tear film-meniscus boundary are subordinate. A suitable value of the diffusion coefficient, D, is given by the diffusivity of sodium chloride in water, which is 2.6e-9 $m^2\,s^{-1}$ (Riquelme et al., 2007; Martinez et al., 2002). Then, for the parameters in Table 1, and using the simulation results of Fig. 5B to estimate the ratio of concentrations, we find the expression on the right of (8) evaluates to about 5e-3. Thus the effects of diffusion are not even one percent of the effects of advection for these parameters. Varying the meniscus radius of curvature, the evaporation rates or the blink frequency as in the main body of the paper, the mean diffusive flux is still never more than four percent of the mean advection flux.

[1] Strictly, this calculation has neglected Taylor dispersion (Taylor, 1953); however, for the lengthscales and timescales associated with the interblink plus the tear film and meniscus, Taylor dispersion is negligible (Guell et al., 1987).

This is also true for all other parameter variations considered, except conceivably when the flux, F, between the tears and meniscus is reduced by an order of magnitude. Then, for large differences between the tear and meniscus compartments, the diffusive and advective fluxes start to become of similar magnitudes, with the right of relation (8) as large as 4/10 for the highest blink rates and the most extreme concentration differences between compartments. However, rather than attempting to further refine the bound in relation (8) to show that diffusion is negligible, this instead can be demonstrated by noting that under such extreme conditions neither the diffusive flux nor the advective flux changes the solute levels in the tear film extensively during the interblink.

Consequently, diffusion at the tear-meniscus boundary can be safely neglected in all the simulations we have performed without impacting on any results. An analogous investigation reveals exactly the same conclusion, that diffusion can be neglected to good approximation, for the meniscus-fornical sac boundary during the interblink. This is an important simplification due to the difficulty with incorporating diffusion into a compartmental model given such transport is driven by time dependent spatial gradients.

References

Adatia, F.A., Michaeli-Cohen, A., Naor, J., Caffery, B., Bookman, A., Slomovic, A., 2004. Correlation between corneal sensitivity, subjective dry eye symptoms and corneal staining in Sjögren's syndrome. Canadian Journal of Ophthalmology 7, 767–771.

Baudouin, C., 2007. The vicious circle in dry eye syndrome: a mechanistic approach. Journal Francais de Ophthalmologie 30, 239–246.

Begley, C.G., Chalmers, R.L., Abetz, L., Venkatataman, K., Mertzanis, P., Caffery, B.A., Snyder, C., Edrington, T., Nelson, D., Simpson, T., 2004. The relationship between habitual patient-reported symptoms and clinical signs among patients with dry eye of varying severity. Investigative Ophthalmology & Visual Science 11, 4753–4761.

Begley, C.G., Himebaugh, N., Renner, D., Liu, H., Chalmers, R., Simpson, T., Varikooty, J., 2006. Tear breakup dynamics: a technique for quantifying tear film instability. Optometry and Vision Science 83, 15–21.

Beuerman, R.W., Mircheff, A.K., Pflugfelder, S.C., Stern, M.E., 2004. The lacrimal functional unit. In: Pflugfelder, S.C., Stern, M.E., Beuerman, R.W. (Eds.), Dry Eye and the Ocular Surface – a Unified Approach. Marcel Dekker, New York, pp. 11–39.

Blehm, C., Vishnu, S., Khattak, A., Mitra, S., Yee, R.W., 2005. Computer vision syndrome, a review. Survey of Ophthalmology 50, 253–262.

Braun, R.J., Fitt, A.D., 2003. Modelling drainage of the precorneal tear film after a blink. Mathematical Medicine and Biology 20, 1–28.

Braun, R.J., King-Smith, P.E., 2007. Model problems for the tear film in a blink cycle: single-equation models. Journal of Fluid Mechanics 586, 465–490.

Bron, A.J., 2001. Diagnosis of dry eye. Survey of Ophthalmology 45 (Suppl. 2), S21–S26.

Bron, A.J., Tiffany, J.M., Yokoi, N., Gouveia, S.M., 2002. Using osmolarity to diagnose dry eye: a compartmental hypothesis and review of our assumptions. Advances in Experimental Medicine and Biology 506, 1087–1095.

Bron, A.J., Yokoi, N., Gaffney, E.A., Tiffany, J.M., 2009. Predicted phenotypes of dry eye – proposed consequences of its natural history. The Ocular Surface 7, 78–92.

Dartt, D.A., 2002. Regulation of mucin and fluid secretion by conjunctival epithelial cells. Progress in Retinal and Eye Research 21, 555–576.

Dartt, D.A., 2005. Regulation of mucin and fluid secretion by conjunctival epithelial cells. Graefe's Archive for Clinical and Experimental Ophthalmology 243, 228–234.

DEWS, 2007a. The definition and classification of dry eye disease: report of the definition and classification subcommittee of the international dry eye workshop (2007). The Ocular Surface 5, 75–92.

DEWS, 2007b. The epidemiology of dry eye disease: report of the epidemiology subcommittee of the international dry eye workshop (2007). The Ocular Surface 5, 93–107.

Dilly, P.N., Guillon, M., McGrogan, L., 1998. Video biomicroscopy of the tear film. Advances in Experimental Medicine and Biology 438, 737–743.

Doane, M.G., 1981. Blinking and the mechanics of the lacrimal drainage system. Ophthalmology 88, 844–851.

Farris, R.L., Stuchell, R.N., Mandel, I.D., 1986. Tear osmolarity variation in the dry eye. Transactions of the American Ophthalmological Society 84, 250–268.

Fraunfelder, F.F., 1976. Extraocular fluid dynamics: how best to apply topical ocular medication. Transactions of the American Ophthalmological Society 74, 457–486.

Gilbard, J.P., 1994. Human tear film electrolyte concentrations in health and dry eye disease. International Ophthalmology Clinics 34, 27–36.

Gilbard, J.P., Carter, J.B., Sang, D.N., Refojo, M.F., Hanninen, L.A., Kenyon, K.R., 1984. Morphologic effect of hyperosmolarity on rabbit corneal epithelium. Ophthalmology 91, 1205–1212.

Gilbard, J.P., Farris, R.L., 1979. Tear osmolarity and ocular surface disease in keratoconjunctivitis sicca. Archives of Ophthalmology 97, 1642–1646.

Gilbard, J.P., Farris, R.L., Santamaria, J., 1978. Osmolarity of tear microvolumes in keratoconjunctivitis sicca. Archives of Ophthalmology 96, 677–681.

Gilbard, J.P., Rossi, S.R., Heyda, K.G., 1989. Tear film and ocular surface changes after closure of the meibomian gland orifices in the rabbit. Ophthalmology 96, 1180–1186.

Goebbels, M., Goebbels, G., Breitbach, R., Spitznas, M., 1992. Tear secretion in dry eye as assessed by objective fluorophotometry. German Journal of Ophthalmology 1, 350–353.

Goto, E., Endo, K., Suzuki, A., Fujikura, Y., Matsumoto, Y., Tsubota, K., 2003. Tear evaporation dynamics in normal subjects and subjects with obstructive meibomian gland dysfunction. Investigative Ophthalmology & Visual Science 44, 533–539.

Goto, E., Tseng, S.C., 2003. Differentiation of lipid tear deficiency dry eye by kinetic analysis of tear interference images. Archives of Ophthalmology 121, 173–180.

Goto, E., Yagi, Y., Matsumoto, Y., Tsubota, K., 2002. Impaired functional visual acuity of dry eye patients. American Journal of Ophthalmology 133, 181–186.

Goto, T., Zheng, X.D., Klyce, S.D., Kataoka, H., Uno, T., Karon, M., Tatematsu, Y., Bessyo, T., Tsubota, K., Ohashi, Y., 2008. A new method for tear film stability analysis using videokeratography. American Journal of Ophthalmology 135, 607–612.

Guell, D.C., Cox, R.G., Brenner, H., 1987. Taylor dispersion in conduits of large aspect ratio. Chemical Engineering Communications 58, 231–244.

Gupta, Y., Gupta, M., Rizvi, S.A.R., Gupta, M., 2006. "Xerosis meter": a new concept in dry eye evaluation. Graefe's Archive for Clinical and Experimental Ophthalmology 244, 9–13.

Harrison, W.W., Begley, C.G., Liu, H., Chen, M., Garcia, M., Smith, J.A., 2008. Menisci and fullness of the blink in dry eye. Optometry and Vision Science 85, 706–714.

Holly, F., Lemp, M.A., 1973. Formation and rupture of the tear film. Experimental Eye Research 15, 515–525.

Huang, A.J.W., Belldegrun, R., Hanninen, L., Kenyon, K.R., Tseng, S.C.G., Refojo, M.F., 1989. Effect of hypertonic solutions on conjunctival epithelium and mucin like glycoprotein discharge. Cornea 8, 15–20.

Johnson, M.E., Murphy, P.J., 2005. The agreement and repeatability of tear meniscus height measurement. Methods, Optometry and Vision Science 82, 1030–1037.

Johnson, M.E., Murphy, P.J., 2006. Temporal changes in the tear menisci following a blink. Experimental Eye Research 83, 517–525.

Khanal, S., Tomlinson, A., McFadyen, A., Diaper, C., Ramaesh, K., 2008. Dry eye diagnosis. Investigative Ophthalmology & Visual Science 49, 1407–1414.

King-Smith, P.E., Fink, B.A., Fogt, N., Nichols, K.K., Hill, R.M., Wilson, G.S., 2000. The thickness of the human precorneal tear film: evidence from reflection spectra. Investigative Ophthalmology & Visual Science 41, 3348–3359.

King-Smith, P.E., Fink, B.A., Hill, R.M., Koelling, K.W., Tiffany, J.M., 2004. The thickness of the tear film. Current Eye Research 29, 357–368.

King-Smith, P.E., Fink, B.A., Nichols, J.J., Nichols, K.K., Hill, R.M., 2006. Interferometric imaging of the full thickness of the precorneal tear film. Journal of the Optical Society of America A – Optics, Image Science and Vision 23, 2097–2104.

King-Smith, P.E., Nichols, J.J., Nichols, K.K., Fink, B.A., Braun, R.J., 2008. Contributions of evaporation and other mechanisms to tear film thinning and break-up. Optometry and Vision Science 85, 623–630.

Kojima, T., Ishida, R., Dogru, M., Goto, E., Takano, Y., Matsumoto, Y., Kaido, M., Ohashi, Y., Tsubota, K., 2004. A new noninvasive tear stability analysis system for the assessment of dry eyes. Investigative Ophthalmology & Visual Science 45, 1369–1374.

Lee, J.B., Ryu, C.H., Kim, J., Kim, E.K., Kim, H.B., 2000. Comparison of tear secretion and tear film instability after photorefractive keratectomy and laser in situ keratomileusis. Journal of Cataract & Refractive Surgery 26, 1326–1331.

Lemp, M.A., 1995. Report of the national eye institute/industry workshop on clinical trials in dry eye. CLAO J. 21, 221–232.

Levin, M.H., Verkman, A.S., 2004. Aquaporin-dependent water permeation at the mouse ocular surface: in vivo microfluorimetric measurements in cornea and conjunctiva. Investigative Ophthalmology & Visual Science 45, 4423–4432.

Liu, H., Begley, C.G., Chalmers, R., Wilson, G., Srinivas, S.P., Wilkinson, J., 2006. Temporal progression and spatial repeatability of tear breakup. Optometry and Vision Science 83, 723–730.

Liu, H., Begley, C., Chen, M., Bradley, A., Bonanno, J., McNamara, N.A., Nelson, J.D., Simpson, T., 2009. A link between tear instability and hyperosmolarity in dry eye. Invest Ophthalmol Vis Sci. 50, 3671–3679.

Liu, Z., Pflugfelder, S.C., 1999. Corneal surface irregularity and the effect of artificial tears in aqueous tear deficiency. Ophthalmology 106, 936–943.

MacDonald, E.A., Maurice, D.M., 1991. The kinetics of tear fluid under the lower lid. Experimental Eye Research 53, 421–425.

Martinez, C.C., Alanis, E.E., Romero, G.G., 2002. Determinacion interferometrica del coeficiente de difusion de NaCl-H_2O, a distintas concentraciones y temperaturas. Energias Renovables y Medio Ambiente 10, 1–8.

McCulley, J.P., Shine, W.E., 2000. Changing concepts in the diagnosis and mismanagement of blepharitis. Cornea 19, 650–658.

McDonald, J.E., Brubaker, S., 1971. Meniscus induced thinning of the tear film. American Journal of Ophthalmology 72, 139–146.

Mishima, S., Gasset, A., Klyce, D., Baum, J., 1966. Determination of tear flow and volume. Investigative Ophthalmology & Visual Science 5, 264–276.

Murube, J., 2006. Tear osmolarity. The Ocular Surface 1, 62–73.

Nakamori, K., Odawara, M., Nakajima, T., Mizutani, T., Tsubota, K., 1997. Blinking is controlled by ocular surface conditions. American Journal of Ophthalmology 124, 24–30.

Nichols, J.J., Mitchell, G.L., King-Smith, P.E., 2005. Thinning rate of the precorneal and prelens tear films. Investigative Ophthalmology & Visual Science 46, 2353–2361.

Nielsen, P.K., Sogaard, K., Skotte, J., Wolkoff, P., 2008. Ocular surface area and human eye blink frequency during VDU work: the effect of monitor position and task. European Journal of Applied Physiology 103, 1–7.
Ousler, G.W., Hagberg, K.W., Schindelar, M., Welch, D., Abelson, M., 2008. The ocular protection index. Cornea 27, 509–513.
Owens, H., Phillips, J.R., 2002. Tear Spreading Rates: Post-blink. Lacrimal Gland, Tear Film, and Dry Eye Syndromes 3: Basic Science and Clinical Relevance, Pts A. & B. Kluwer Academic/Plenum Pub, New York, pp. 1201–1204.
Pavlidis, M., Stupp, T., Grenzebach, U., Busse, H., Thanos, S., 2002. Ultrasonic visualization of the effect of blinking on the lacrimal pump mechanism. Progress in Retinal and Eye Research 21, 555–576.
Pflugfelder, S.C., Jones, D., Ji, Z.H., Afonso, A., Monroy, D., 1999. Altered cytokine balance in the tear fluid and conjunctiva of patients with Sjögren's syndrome keratoconjunctivitis sicca. Current Eye Research 19, 201–211.
Pflugfelder, S.C., Solomon, A., Stern, M.E., 2000. The diagnosis and management of dry eye – a twenty-five-year review. Cornea 19, 644–649.
Prydal, J.I., Artal, P., Woon, H., Campbell, F.W., 1992. Study of human precorneal tear film thickness and structure using laser interferometry. Investigative Ophthalmology & Visual Science 33, 2006–2011.
Rieger, G., 1992. The importance of the precorneal tear film for the quality of optical imaging. British Journal of Ophthalmology 76, 157–158.
Riquelme, R., Lira, I., Pierez-Liopez, C.S., Rayas, J.A., Rodriguez-Vera, R., 2007. Interferometric measurement of a diffusion coefficient: comparison of two methods and uncertainty analysis. Journal of Physics D: Applied Physics 40, 2769–2776.
Rolando, M., Refojo, M.F., 1983. Tear evaporimeter for measuring water evaporation rate from the tear film under controlled conditions in humans. Experimental Eye Research 36, 25–33.
Sharma, A., Tiwari, S., Khanna, R., Tiffany, J.M., 1998. In: Sullivan, D., et al. (Eds.), Lacrimal Gland, Tear Film, and Dry Eye Syndromes 2. Plenum Press, NY.
Shimazaki, J., Goto, E., Ono, M., Shimmura, S., Tsubota, K., 1998. Meibomian gland dysfunction in patients with Sjögren syndrome. Ophthalmology 105, 1485–1488.
Stern, M.E., Beuerman, R.W., Fox, R.I., Gao, J.P., Mircheff, A.K., Pflugfelder, S.C., 1998a. The pathology of dry eye: the interaction between the ocular surface and lacrimal glands. Cornea 17, 584–589.
Stern, M.E., Beuerman, R.W., Fox, R.I., Gao, J.P., Mircheff, A.K., Pflugfelder, S.C., 1998b. A unified theory of the role of the ocular surface in dry eye. Advances in Experimental Medicine and Biology 438, 643–651.
Stern, M.E., Gao, J., Siemasko, K.F., Beuerman, R.W., Pflugfelder, S.C., 2004. The role of the lacrimal functional unit in the pathophysiology of dry eye. Experimental Eye Research 78, 409–416.
Taylor, G.I., 1953. Dispersion of soluble matte; in solvent flowing slowly through a tube. Proceedings of the Royal Society A 219, 186–203.
Tiffany, J.M., Todd, B.S., Baker, M.R., 1997. Calculation of the exposed area of the human eye. Investigative Ophthalmology & Visual Science 38, 766.
Tomlinson, A., Blades, K.J., Pearce, E.I., 2001a. What does the phenol red thread test actually measure? Optometry and Vision Science 78, 142–146.
Tomlinson, A., Pearce, E.I., Simmons, P.A., Blades, K., 2001b. Effect of oral contraceptives on tear physiology. Ophthalmic and Physiological Optics 21, 9–16.
Tomlinson, A., Khanal, S., 2005. Assessment of tear film dynamics quantification approach. The Ocular Surface 3, 81–95.
Tomlinson, A., Khanal, S., Ramaesh, K., Diaper, C., McFadyen, A., 2006. Tear film osmolarity: determination of a referent for dry eye diagnosis. Investigative Ophthalmology & Visual Science 47, 4309–4315.
Tsubota, K., 1989. The effect of wearing spectacles on the humidity of the eye. American Journal of Ophthalmology 108, 92–93.
Tsubota, K., 1998. Tear dynamics and dry eye. Progress in Retinal and Eye Research 17, 565–596.
Tsubota, K., Fujihara, T., Saito, K., Takeuchi, T., 1999. Conjunctival epithelium expression of hla-dr in dry eye patients. Ophthalmologica 213, 16–19.
Tsubota, K., Hata, S., Okusawa, Y., Egami, F., Ohtsuki, T., Nakamori, K., 1996. Quantitative videographic analysis of blinking in normal subjects and patients with dry eye. Archives of Ophthalmology 114, 715–720.
Tsubota, K., Nakamori, K., 1995. Effects of ocular surface area and blink rate on tear dynamics. Archives of Ophthalmology 113, 155–158.
Vitale, S., Goodman, L.A., Reed, G.F., Smith, J.A., 2004. Comparison of the NEI-VFQ and OSDI questionnaires in patients with Sjögren's syndrome-related dry eyes. Health and Quality of Life Outcomes 2, 44.
Wong, H., Fatt, I., Radke, C.J., 1996. Deposition and thinning of the human tear film. Journal of Colloid and Interface Science 184, 44–51.
Worakul, N., Robinson, J.R., 1997. Ocular pharmacokinetics/pharmacodynamics. European Journal of Pharmaceutics and Biopharmaceutics 44, 71–83.
Yokoi, N., Bron, A.J., Tiffany, J.M., Brown, N., Hsuan, J., Fowler, C., 1999. Reflective meniscometry: a. Non-invasive method to measure tear meniscus curvature. British Journal of Ophthalmology 83, 92–97.
Yokoi, N., Bron, A.J., Tiffany, J.M., Maruyama, K., Komuro, A., Kinoshita, S., 2004. Relationship between tear volume and tear meniscus curvature. Archives of Ophthalmology 122, 1265–1269.
Zhu, H., Chauhan, A., 2005a. A mathematical model for ocular tear and solute balance. Current Eye Research 30, 841–854.
Zhu, H., Chauhan, A., 2005b. A mathematical model for tear drainage through the canaliculi. Current Eye Research 30, 621–630.
Zhu, H., Chauhan, A., 2007. Tear dynamics model. Current Eye Research 32, 177–197.

Glossary

Advection (advective): Fluid flow (associated with fluid flow).
Aspect Ratio: The ratio of the smallest spatial lengthscale to the largest.
Capillary Forces: Forces due to *surface tension*.
Centroid: The centre of an irregular object; if the object is two dimensional and of uniform density, it is the point where the object will balance on a pin-head.
Elastic Modulus: An object's tendency to be deformed; the reciprocal of stiffness.
Flux: A measure of flow or *transport*. In physics it is typically the rate at which particles are, or fluid or energy is, transported through a unit surface area. Here it is a measure of transport of fluid or solutes between compartments.
Order of Magnitude: A factor of ten.
Parameter: A pre-assigned physical quantity that will not change during the blink or interblink. All model inputs are parameters.
Radius Of Curvature: The radius of a circle that locally asymptotes to a curve; it thus measures curvature.
Surface Tension: Forces that exist at an interface between two fluids, for example air and water. It will typically act to reduce interface curvature.
Taylor Dispersion: An augmented solute transport due to a combination of diffusion and shearing flow when advective transport dominates (Taylor, 1953).
Transport: Movement of solutes or fluid.
Variable: A biophysical quantity in the model that will typically change during the blink–interblink cycle; these are model predictions.
Viscosity: A measure of the extent a fluid resists shearing.